Article

Cell Metabolism

Separate gut-brain circuits for fat and sugar reinforcement combine to promote overeating

Graphical abstract

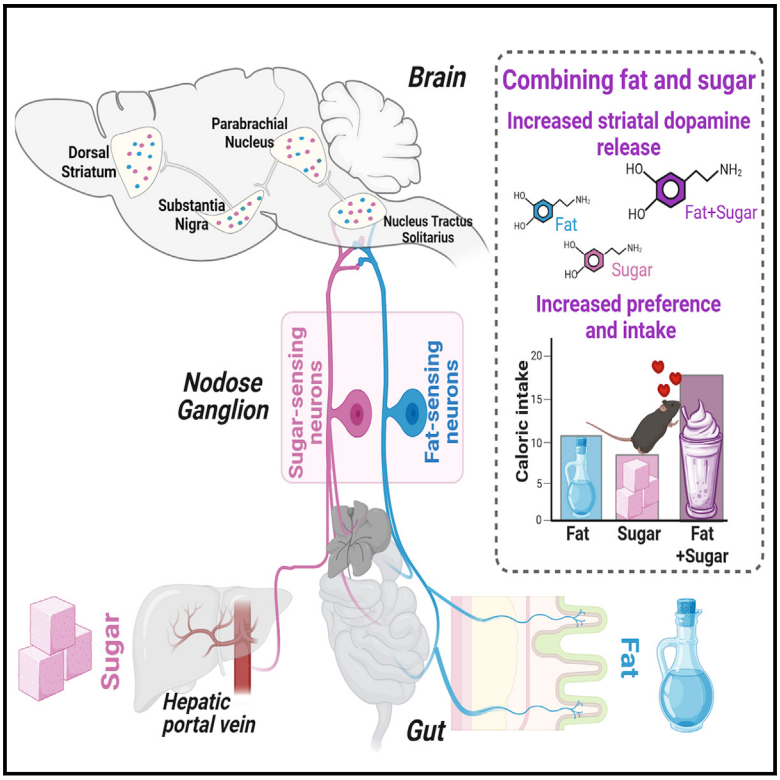

Highlights

- Intestinal fats and sugars are sensed by distinct vagal populations
- Nutrient-sensing vagal sensory neurons are necessary and sufficient for reinforcement
- Both fat and sugar cause dopamine release by engaging separate central reward circuits
- Combining fat and sugar supra-additively increases dopamine efflux and eating

Authors

Molly McDougle, Alan de Araujo, Arashdeep Singh, ..., Nikhil Urs, Brandon Warren, Guillaume de Lartigue

Correspondence

gdelartigue@monell.org

In brief

McDougle et al. unveil gut-brain circuits for sugar and fat consumption. Separate chemosensory vagal neurons respond to either post-ingestive fat or sugar and engage distinct but parallel downstream reward circuits, crucial for reinforcement. Foods combining fats and sugars simultaneously recruit both circuits promoting the subconscious drive to overeat obesogenic diets.

McDougle et al., 2024, Cell Metabolism *36*, 1–15
February 6, 2024 © 2023 The Authors. Published by Elsevier Inc.
https://doi.org/10.1016/j.cmet.2023.12.014

CellPress

Please cite this article in press as: McDougle et al., Separate gut-brain circuits for fat and sugar reinforcement combine to promote overeating, Cell Metabolism (2023), https://doi.org/10.1016/j.cmet.2023.12.014

Cell Metabolism

CellPress

Article

Separate gut-brain circuits for fat and sugar reinforcement combine to promote overeating

Molly McDougle,[1,2,4] Alan de Araujo,[1,2] Arashdeep Singh,[1,2,3,4] Mingxin Yang,[1,2,3,4] Isadora Braga,[1,3,4] Vincent Paille,[3,4,5] Rebeca Mendez-Hernandez,[3,4] Macarena Vergara,[1,2] Lauren N. Woodie,[6] Abhishek Gour,[7] Abhisheak Sharma,[7] Nikhil Urs,[8] Brandon Warren,[1] and Guillaume de Lartigue[1,2,3,4,9,*]

[1]Department of Pharmacodynamics, University of Florida, Gainesville, FL, USA
[2]Center for Integrative Cardiovascular and Metabolic Disease, University of Florida, Gainesville, FL, USA
[3]Monell Chemical Senses Center, Philadelphia, PA, USA
[4]Department of Neuroscience, University of Pennsylvania, Philadelphia, PA, USA
[5]UMR1280 Physiopathologie des adaptations nutritionnelles, INRAE, Institut des maladies de l'appareil digestif, Université de Nantes, Nantes, France
[6]Institute for Diabetes, Obesity and Metabolism, University of Pennsylvania, Philadelphia, PA, USA
[7]Department of Pharmaceutics, University of Florida, Gainesville, FL, USA
[8]Department of Pharmacology, University of Florida, Gainesville, FL, USA
[9]Lead contact
*Correspondence: gdelartigue@monell.org
https://doi.org/10.1016/j.cmet.2023.12.014

SUMMARY

Food is a powerful natural reinforcer that guides feeding decisions. The vagus nerve conveys internal sensory information from the gut to the brain about nutritional value; however, the cellular and molecular basis of macronutrient-specific reward circuits is poorly understood. Here, we monitor *in vivo* calcium dynamics to provide direct evidence of independent vagal sensing pathways for the detection of dietary fats and sugars. Using activity-dependent genetic capture of vagal neurons activated in response to gut infusions of nutrients, we demonstrate the existence of separate gut-brain circuits for fat and sugar sensing that are necessary and sufficient for nutrient-specific reinforcement. Even when controlling for calories, combined activation of fat and sugar circuits increases nigrostriatal dopamine release and overeating compared with fat or sugar alone. This work provides new insights into the complex sensory circuitry that mediates motivated behavior and suggests that a subconscious internal drive to consume obesogenic diets (e.g., those high in both fat and sugar) may impede conscious dieting efforts.

INTRODUCTION

The sharp rise in global obesity rates has been attributed to changes in the food environment that promote overconsumption of palatable calorie-dense foods that are rich in fats and sugars.[1,2] Animal studies indicate that although palatability guides food choice, it is neither necessary[3–5] nor sufficient[6] to increase food intake. Instead, flavor preferences are rapidly learned as a conditioned response to post-ingestive nutritive cues.[7–10] Thus, orosensory features of food are secondary to its nutritional value in underlying reinforcement.[11] Importantly, the reinforcing value of intragastric infusions of fats or sugars enhance the overall intake of associated flavors.[12–14] Thus, fats and sugars may cause overeating via a mechanism involving post-ingestive signaling, although the relative importance of individual macronutrients in diet-induced weight gain remains hotly debated.[1,15–17] We reasoned that defining the neural mechanisms for macronutrient-specific post-ingestive reinforcement is of critical importance to understanding overeating.

The striatal regions of the basal ganglia are evolutionarily conserved brain substrates responsible for goal-directed behavior. Gustatory stimuli in the oral cavity recruit mesolimbic circuits that release dopamine in the ventral striatum, whereas nutritive stimuli that reach the intestine result in nigrostriatal dopamine release in the dorsal striatum (DS).[18,19] Importantly, recruitment of the nigrostriatal circuit by post-ingestive stimuli occurs independently of palatability,[5,18] which presumably ensures prioritization of calories over flavor. Dopamine release from the substantia nigra pars compacta (SNc) onto the DS is critical for feeding. Genetic deletion of dopamine causes aphagia; however, normal eating behavior can be restored by reintroducing dopamine selectively in the DS.[20,21] Vagal sensory neurons have recently been identified as a key component of a multi-synaptic circuit linking the gut to nigrostriatal dopamine release.[22] Optical stimulation of gut-innervating vagal sensory neurons is reinforcing, and animals actively seek stimuli that engage this circuit.[22] We aim to address whether fats and sugars recruit vagal sensory neurons and whether they engage overlapping or separate circuits.

This is an open access article under the CC BY-NC license (http://creativecommons.org/licenses/by-nc/4.0/).

Please cite this article in press as: McDougle et al., Separate gut-brain circuits for fat and sugar reinforcement combine to promote overeating, Cell Metabolism (2023), https://doi.org/10.1016/j.cmet.2023.12.014

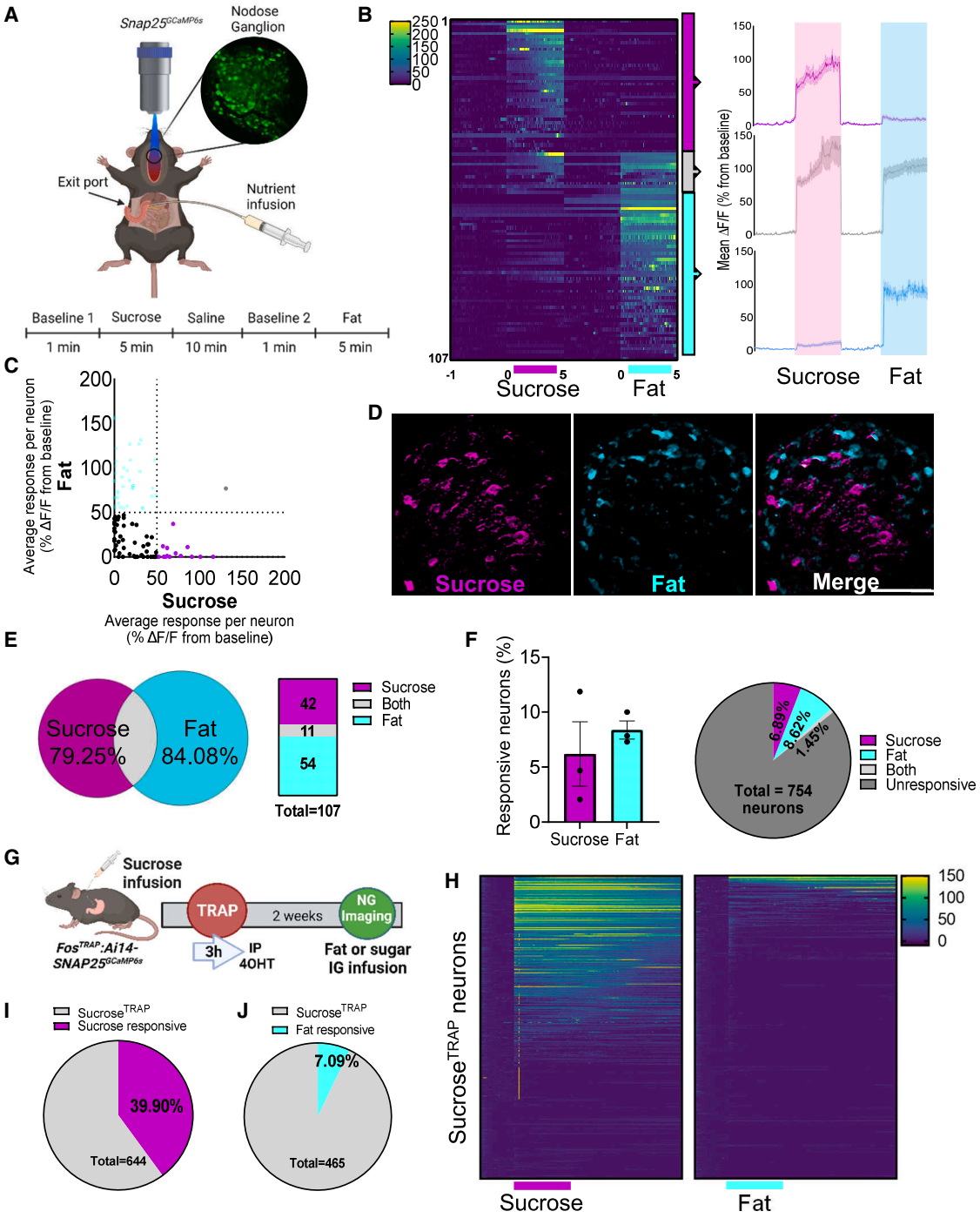

Figure 1. Sucrose and fat activate distinct vagal populations in the nodose ganglia

(A) *In vivo* imaging of the activity pattern of vagal sensory neurons in response to intraduodenal sucrose or fat infusions in *Snap25*-GCaMP6s mice.

(B) Heatmaps depicting time-resolved responses (ΔF/F) of right NG neurons identified as sucrose responders (magenta bar, 5 min) or fat responders (cyan bar, 5 min); On the right, average ΔF/F of GCaMP6s signals in neurons that were responsive to sucrose (magenta), fat (cyan), or both (gray). The shaded areas (pink and blue) represent duration of stimuli. Dark lines represent means and lighter shaded areas represent SEM.

(C) Average ΔF/F of GCaMP6s signal of right NG neurons in response to fat over sucrose; each dot represents a neuron that had at least one peak response of 50% or more above the baseline during the intraduodenal infusions; magenta dots, sucrose responsive; cyan dots, fat responsive; gray dots, responsive to both stimuli; black dots, average response was below 50%.

(D) Image of the nodose ganglion of *Snap25*-GCaMP6s mice showing calcium fluorescence responses to sucrose (magenta) and fat infusion (cyan). Scale bars, 100 μm. N = 3 mice.

(E) Quantification of (D).

(legend continued on next page)

Please cite this article in press as: McDougle et al., Separate gut-brain circuits for fat and sugar reinforcement combine to promote overeating, Cell Metabolism (2023), https://doi.org/10.1016/j.cmet.2023.12.014

Gastrointestinal (GI) infusion of fats[23] or sugars[24] activate the vagus nerve and cause DS dopamine efflux,[25,26], yet previous attempts to address the role of the vagus nerve in appetition have yielded mixed results.[25,27–30] Because vagal sensory neurons are molecularly heterogeneous[31–33] and play a role in diverse physiological functions,[34,35] we reasoned that previously used chemical or surgical lesioning approaches that interrupt global vagal activity lack the specificity required to test the role of distinct vagal sensory populations in nutrient reinforcement. To overcome this problem, we applied virally delivered molecular tools to the nodose ganglia (NG) of Fos^{TRAP} mice to manipulate neuronal populations of the vagus nerve that are activated in response to gastric infusions of sugar or fat. Our results indicate that sugar and fat are sensed by discrete neurons of the vagus nerve and engage parallel but distinct reward circuits to control nutrient-specific reinforcement.

RESULTS

Fats and sugars are sensed by distinct vagal populations

Fats[23] and sugars[24] both increase vagal firing in nerve recording experiments; however, it remains unknown whether different subpopulations of vagal neurons sense specific macronutrients. To address this question, we first adapted a technique for *in vivo* imaging of NG neurons (Figure 1A)[33] using mice expressing the Ca^{2+} indicator GCaMP6s driven by the pan-neuronal promoter *Snap25*.[36,37] We used two-photon microscopy coupled with an electrically tunable lens to record from nodose ganglion tissue in response to duodenal infusion of sugar (sucrose) or fat (corn oil) in the same live animal. A catheter was inserted into the duodenal bulb and an exit port was created 2 cm from the pylorus to restrict the delivery of macronutrient solutions to the proximal intestine (Figure 1A). Analysis of individual neuronal responses indicated that spatially defined vagal neuron subsets are activated in response to different nutrient stimuli (Figures 1B and 1C). NG neurons exhibit either a strong response to fat or a strong response to sugar, with few neurons responding to both (Figures 1C–1F). Notably, these intestinal nutrient-sensitive neurons accounted for a small fraction of the total population (~17%, Figure 1F), supporting the concept of high cellular division of function within NG.[32]

Previous findings indicate that the right NG is connected to a nigrostriatal circuit and required for fat reinforcement.[22] Therefore, we next used animals with an intact gut to record vagal sensory neuron activity from the right NG in response to intragastric infusion of equicaloric concentrations of sucrose (15%) or fat (6.8%, Figures S1A–S1C), administered over 5 min based on the ingestion rate during natural ingestive behavior (Figure S1D). NG neurons remain active for over 15 min in response to either sucrose or fat in the animals (Figures S1A and S1B). As expected, recordings from the left NG showed fewer nutrient-responsive neurons than the right NG (Figure S1E). Compared with intraduodenal infusions, intragastric infusion postponed peak NG neural activity (Figures S1F–S1I), presumably caused by delayed gastric emptying.[38,39] These data support previous evidence that the proximal intestine is the first site of post-ingestive nutrient sensing.[40]

To confirm that distinct NG populations sense different macronutrients, we used a transgenic mouse line that allows targeted recombination in active populations (TRAP2)[41,42] (Figure 1G). These mice express an inducible Cre recombinase, iCreER^{T2}, under the control of an activity-dependent *Fos* promoter (Fos^{TRAP} mice), enabling permanent genetic access to neuronal populations based on their activation to a defined, time-constrained stimulus when paired with injection of 4-hydroxytamoxifen (4-OHT).[27,43,44] We crossed the Fos^{TRAP} mice with a Cre-dependent tdTomato reporter line, Ai14,[45] and demonstrated that the majority of sugar-TRAP NG neurons increase calcium fluorescence in response to gastric infusions of sucrose (15% w/v, Figures 1H and 1I). However, sugar-TRAP neurons showed little activity in response to equicaloric infusion of intragastric fat (6.8% v/v, Figures 1H and 1J).

Targeting nutrient-specific gut-brain pathways using Fos^{TRAP}

Although food is consumed orally under physiological conditions, we infused foods directly into the stomach to bypass the oral cavity and address how post-ingestive stimuli reinforce food intake independently of taste. We confirmed that tdTomato^{+} NG neurons increased in response to intragastric infusion of sugar (sucrose, 15% w/v, Sugar^{TRAP}) or equicaloric fat (intralipid, 6.8% w/v, Fat^{TRAP}) compared with iso-osmotic saline (Saline^{TRAP}) (Figures 2A–2D). Comparisons of neural activity in response to nutrient concentrations suggest that there is a dose-dependent response at the level of both the NG (Figures S1J and S1K) and nucleus tractus solitarius (NTS; Figures S1L and S1M). These data clearly indicate that fats and sugars recruit separate peripheral vagal circuits that convey information about the type, and possibly concentration, of nutrients from the gut to the brain.

Neurons of the NTS, which receive vagal inputs, had similarly increased tdTomato labeling in response to intragastric infusion of either fat or sugar compared with controls (Figures S1N and S1O) and increased in a dose-responsive manner (Figures S1K and S1L). These findings are consistent with nutrient-induced Fos staining in the NTS.[46–48] To validate the specificity of the Fos^{TRAP} approach to target macronutrient sensing populations, we confirm that tdTomato labeling is dependent on 4-OHT (Figures S1N and S1O), and we demonstrate that there is high overlap between Fos^{TRAP} labeling and Fos immunoreactivity in response to the same stimulus (Figures S1P–S1T).

The potent GI stimulus cholecystokinin (CCK, i.p.) was used because it is known to robustly inhibit food intake by acting on CCKa receptors (CCKaR) expressed by vagal sensory neurons,[49] and we reasoned that intraperitoneal injections would maximize reproducibility compared with intragastric infusions that are dependent on a number of uncontrolled variables (e.g.,

(F) Percentage of nodose ganglia neurons that were responsive to intraduodenal infusions of sucrose and fat. Data are presented as mean ± SEM.
(G) Schematic of Fos^{TRAP}: Ai14 x *Snap25*-GCAMP6s triple transgenic mice, have tdTomato labeling of sucrose responsive neurons and real-time neural activity of NG neurons are recorded in response to intragastric infusion of equicaloric sugar or fat.
(H) Heatmaps depicting time-resolved responses (ΔF/F) of sucrose^{TRAP} neurons following sucrose infusion (magenta bar) or fat infusion (blue bar).
(I and J) Percentage of sucrose^{TRAP} NG neurons that were active in response to gastric infusions of sucrose or (J) equicaloric gastric infusions of fat. N = 4–5 mice.

Please cite this article in press as: McDougle et al., Separate gut-brain circuits for fat and sugar reinforcement combine to promote overeating, Cell Metabolism (2023), https://doi.org/10.1016/j.cmet.2023.12.014

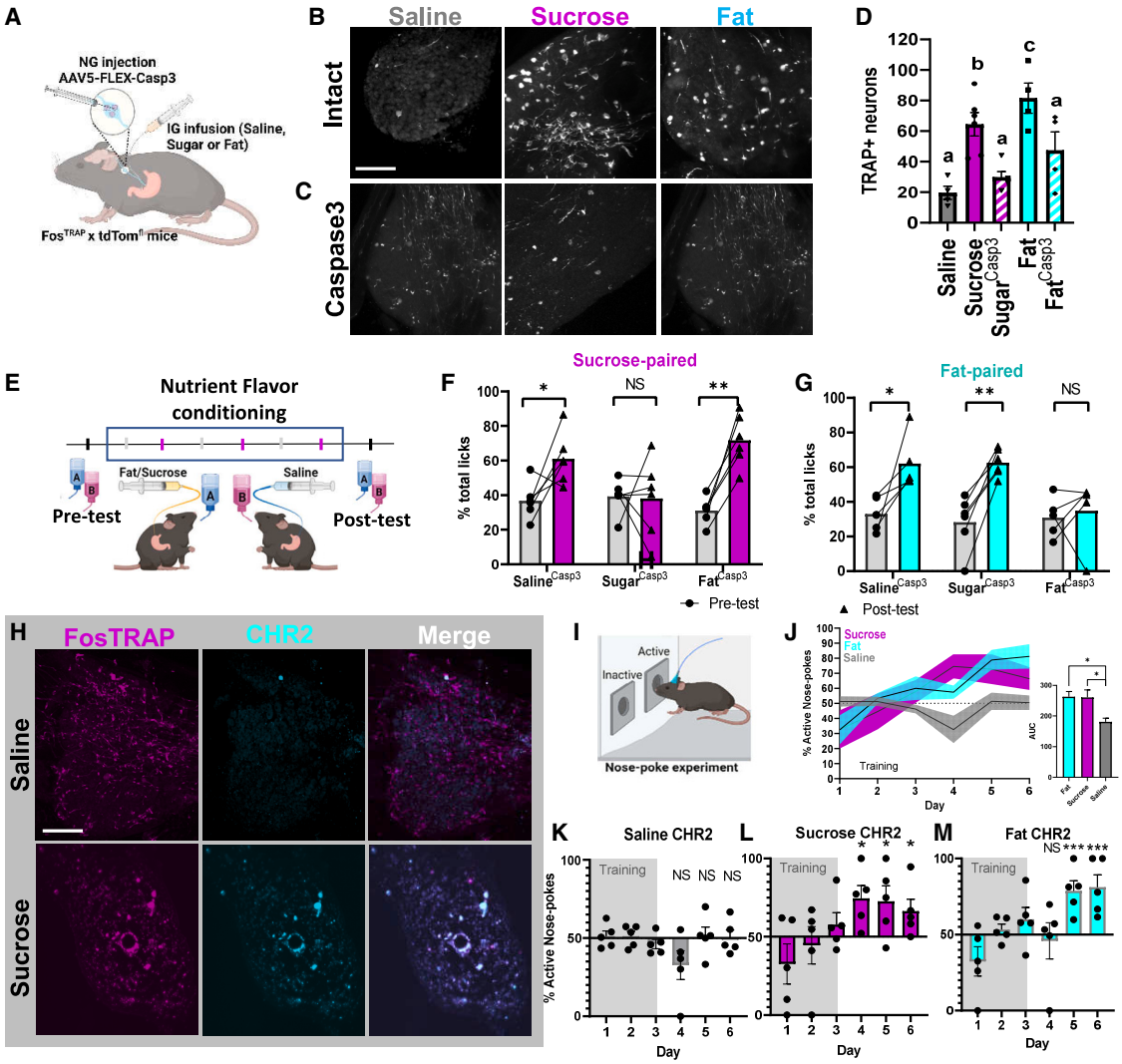

Figure 2. Sucrose and fat promote reinforcement via distinct vagal sensory populations

(A) Schematic of the Fos^{TRAP} approach to selectively ablate vagal sensory neurons that respond to intragastric infusion of fat or sugar.

(B and C) Representative image of nodose ganglia neurons from Fos^{TRAP} mice following intagastric infusion of saline, sucrose, of fat, or saline in the absence (B) or presence (C) of viral-mediated caspase ablation.

(D) Quantification of (B) and (C) showing increased tdTomato labeling in NG neurons in response to sucrose or fat infusions compared with saline and confirming deletion of tdTomato neurons n = 4–6. One-way ANOVA with Tukey post hoc analysis.

(E) Diagram demonstrating the flavor-nutrient conditioning paradigm.

(F) Conditioning increases preference for the flavor paired with intragastic sucrose in Saline^{TRAP} and Fat^{TRAP} mice but does not occur in Sugar^{TRAP} mice n = 5–6. Two-way ANOVA with Holm-Sidak post hoc analysis.

(G) Conditioning increases preference for the flavor paired with intragastic fat in Saline^{TRAP} and Sugar^{TRAP} mice but does not occur in Fat^{TRAP} mice n = 5–6. Two-way ANOVA with Holm-Sidak post hoc analysis.

(H) Representative images of ChR2 construct targeted to NG of Fos^{TRAP} mice.

(I) Mice were trained in a nose-poke induced optogenetic self-stimulation paradigm.

(J) After 3 days of training with food pellets in both nose holes with active hole triggering optogenetic stimulation, the mice in the Fat^{TRAP} and Sugar^{TRAP} groups learned to favor the active nose hole. One-way ANOVA with Dunnett's multiple comparisons test.

(K–M) Individual mouse data confirming that Saline^{TRAP} mice (K) failed to learn to self-stimulate while Sugar^{TRAP} (L) and Fat^{TRAP} (M) mice learned to nose poke for vagal stimulation n = 5. One-way ANOVA with Holm-Sidak post hoc analysis. Data are presented as mean ± SEM. *p < 0.05, **p < 0.01, ***p < 0.001, NS, not significant.

motility, digestion, and absorption rates). TdTomato^{+} NTS neurons faithfully overlap with Fos-positive cells in response to CCK (Figures S1P–S1R). By contrast, few tdTomato-labeled CCK^{TRAP} NTS neurons were double labeled with Fos immunoreactivity after saline injection (Figures S1S and S1T). These results highlight the specificity and selectivity of the Fos^{TRAP} approach and that we can efficiently and reliably gain genetic access to NG neurons that sense either fat or sugar.

Please cite this article in press as: McDougle et al., Separate gut-brain circuits for fat and sugar reinforcement combine to promote overeating, Cell Metabolism (2023), https://doi.org/10.1016/j.cmet.2023.12.014

CellPress

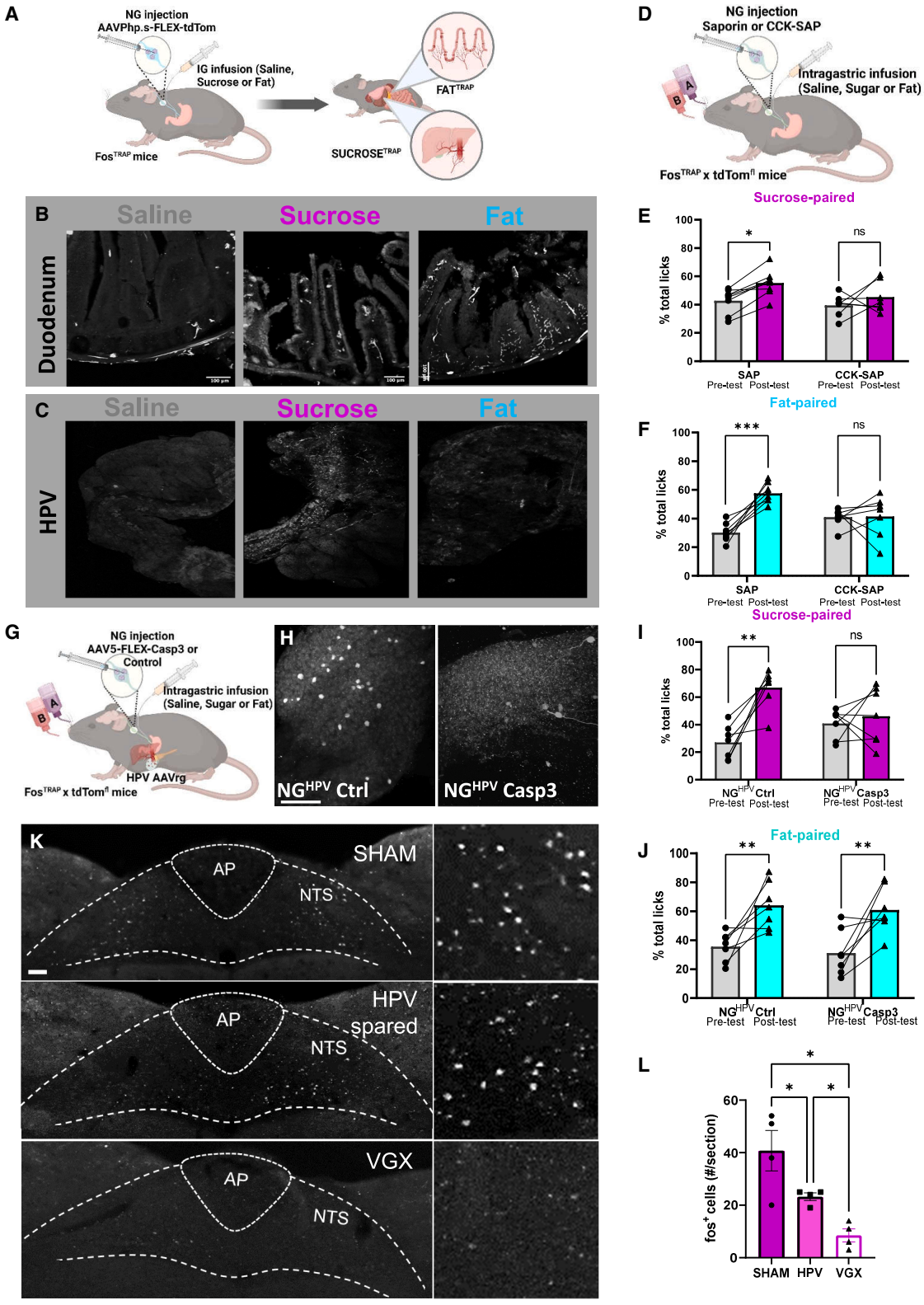

Figure 3. Anatomical dissociation of peripheral projections of sucrose- and fat-responsive NG neurons

(A) Schematic of viral guided mapping of vagal sensory neuron projections by injecting AAV-DIO-tdTomato virus bilaterally into NG of Fos^{TRAP} mice in response to intragastric saline, sucrose (15%), or fat (6.8%).

(B) Terminals visualized by immunofluorescence of the duodenum are most abundant in Fat^{TRAP} mice. n = 4.

(legend continued on next page)

Please cite this article in press as: McDougle et al., Separate gut-brain circuits for fat and sugar reinforcement combine to promote overeating, Cell Metabolism (2023), https://doi.org/10.1016/j.cmet.2023.12.014

Sugar- and fat-sensing NG neurons are necessary and sufficient for macronutrient-specific reinforcement

Having validated the Fos^{TRAP} approach, we assessed the necessity of separate macronutrient-sensitive vagal sensory populations for food reinforcement. As a measure of nutrient reinforcement, we performed a flavor-nutrient conditioning task, in which animals are trained to prefer a novel flavor that has been experimentally paired with an intragastric infusion of nutrients (Figure 2E). Fos^{TRAP} mice received bilateral NG injections of the viral construct AAV-flex-taCasp3-TEVp[50] (Figure 2C and 2D), which enables selective ablation of vagal sensory neurons responsive to fat or sugar during the TRAP protocol. To confirm that viral injection of NG alone, prior to trapping, had no effect on post-ingestive reinforcement, we trained mice to associate flavors with either intragastric fat or sugar. As expected,[13,14] these mice were able to form a conditioned preference for each macronutrient (Figures S2A–S2C). Next, the TRAP protocol was performed to ablate the nutrient-responsive populations. Mildly fasted Fos^{TRAP} mice were separated into 3 groups that received intragastric infusions (500 μL and 100 μL/min) of either saline, sugar (sucrose, 15% w/v), or equicaloric fat (microlipid, 6.8% v/v), followed by i.p. 4-OHT (30 μg/kg). This protocol deleted vagal sensory neurons based on their nutrient-responsive profile (Figures 2C and 2D) while leaving other sensory and motor neurons intact. Control Saline^{TRAP} mice still formed robust preferences for novel, non-nutritive flavors paired with either intragastric infusion of sugar or fat. Conversely, Fat^{TRAP} mice with deletion of fat-sensing NG neurons formed normal preference for the flavor paired with sugar but failed to reinforce the flavor paired with fat, whereas Sugar^{TRAP} mice with deletion of sucrose sensing NG neurons had selectively abolished sugar reinforcement (Figures 2F and 2G). These striking findings demonstrate that separate, mutually exclusive populations of vagal sensory neurons independently drive sugar or fat reinforcement.

To assess whether stimulation of fat- or sugar-sensing vagal neurons is each independently sufficient for reinforcement, mice underwent a previously validated self-stimulation behavioral task[22] in which optogenetic stimulation of vagal sensory terminals is paired to nose poke (Figure 2I). Fos^{TRAP} mice received bilateral NG injection of the *Cre*-inducible viral construct AAV9-EF1a-DIO-hChR2 (H134R)-EYFP (ChR2)[51] to selectively express the light-sensitive depolarizing channel channelrhodopsin-2 (ChR2) in vagal sensory neurons (Figure 2H). An optic fiber was placed above vagal terminals in the medial NTS,[22,52] and ChR2 expression in NG neurons was enabled by trapping with intragastric fat, sugar, or saline. Optogenetic activation of vagal terminals from Sugar^{TRAP} mice increased Fos expression throughout the NTS compared with control Saline^{TRAP} mice (Figures S2C and S2D). Saline^{TRAP} mice (Figure 2K) did not learn to prefer the nose hole that triggers optogenetic stimulation of vagal terminals. In contrast, both Sugar^{TRAP} (Figure 2L) and Fat^{TRAP} (Figure 2M) mice that express ChR2 in NG learned to self-stimulate vagal terminals, a hallmark behavior of reward.[53,54] Together, these findings reveal that separate vagal circuits are both necessary and sufficient for the development of macronutrient-specific reinforcement.

Sugar- and fat-responsive NG neurons innervate different organs

Based on the evidence that sugars and fats are signaled from different vagal populations, we next wanted to determine the site of sugar and fat reinforcement. We used genetic guided anatomical tracing of sugar- or fat-responsive vagal afferent fibers by injecting the Cre-dependent virus AAVPhp.S-Flex-tdTomato bilaterally into NG of Fos^{TRAP} mice (Figure 3A). Striking differences in peripheral innervation patterns were observed between sugar- and fat-sensing vagal populations. In the duodenum, we observed extensive innervation of mucosal endings in intestinal villi from Sugar^{TRAP} mice and Fat^{TRAP} mice, but not Saline^{TRAP} mice (Figure 3B). Furthermore, we observed abundant vagal-derived tdTomato^{+} fibers running along the portal blood vessels from Sugar^{TRAP} mice (Figure 3C), but not in Fat^{TRAP} or Saline^{TRAP} mice. These data suggest that the duodenum is a key sensing site for both sugar- and fat-sensing, but sugar-sensing also occurs at the level of the hepatic portal vein (HPV).

To assess the importance of the GI vagal fibers for fat signaling, we injected the neurotoxin saporin conjugated to CCK (CCK-SAP) bilaterally into the NG of wild-type (WT) mice (Figures 3D and S3A), a previously validated method for selective vagal deafferentation of the upper GI tract.[55] As predicted from the viral-tracing experiments, vagal deafferentation of the upper gut using CCK-SAP treatment blocked the reinforcement of both sugar and fat (Figures 3E and 3F) in mice with confirmed CCK-SAP deafferentation (Figure S3B).

CCK-SAP significantly increased the oral consumption of 6.8% fat solution (Figure S3C), with no change in the intake of equicaloric sucrose solution (Figure S3D). These data are consistent with evidence that vagal deafferentation of the gut abolishes fat, but not sugar, satiety in rats[56]; instead, sugars may inhibit hunger via a spinal gut-brain circuit.[57] Consistent with these findings, *Cckar* is co-expressed in ~75% of both Sugar^{TRAP} (Figures S3E–S3G) and Fat^{TRAP} NG

(C) The hepatic portal vein exclusively receives innervation from Sugar^{TRAP} mice. n = 4.
(D) Schematic of approach for vagal deafferentation of the gut using CCK-SAP.
(E) CCK-SAP treatment abolishes flavor conditioning in response to intragastric infusion sucrose. n = 7–8. Two-way ANOVA with Holm-Sidak post hoc analysis.
(F) CCK-SAP treatment abolishes flavor conditioning in response to intragastric infusion fat. n = 7–8. Two-way ANOVA with Holm-Sidak post hoc analysis.
(G) Combinatorial viral approach for vagal deafferentation of the HPV.
(H) Representative images of labeling in a subsets of NG neurons innervating the HPV can be selectively ablated.
(I and J) Loss of NG^{HPV} neurons abolishes sucrose (I) but not fat (J) reinforcement. n = 7.
(K) Representative images of Fos expression in the NTS following intragastric sucrose infusion (15%) in mice with subdiaphragmatic vagotomy with or without sparing of the hepatic branch, or sham controls.
(L) Quantification demonstrating NTS Fos in response to sucrose is blunted by SDV but partial restoration when the hepatic branch is spared. One-way ANOVA with Holm-Sidak post hoc analysis. Data are presented as mean ± SEM. *p < 0.05, **p < 0.01, ***p < 0.001, NS, not significant.

Please cite this article in press as: McDougle et al., Separate gut-brain circuits for fat and sugar reinforcement combine to promote overeating, Cell Metabolism (2023), https://doi.org/10.1016/j.cmet.2023.12.014

CellPress

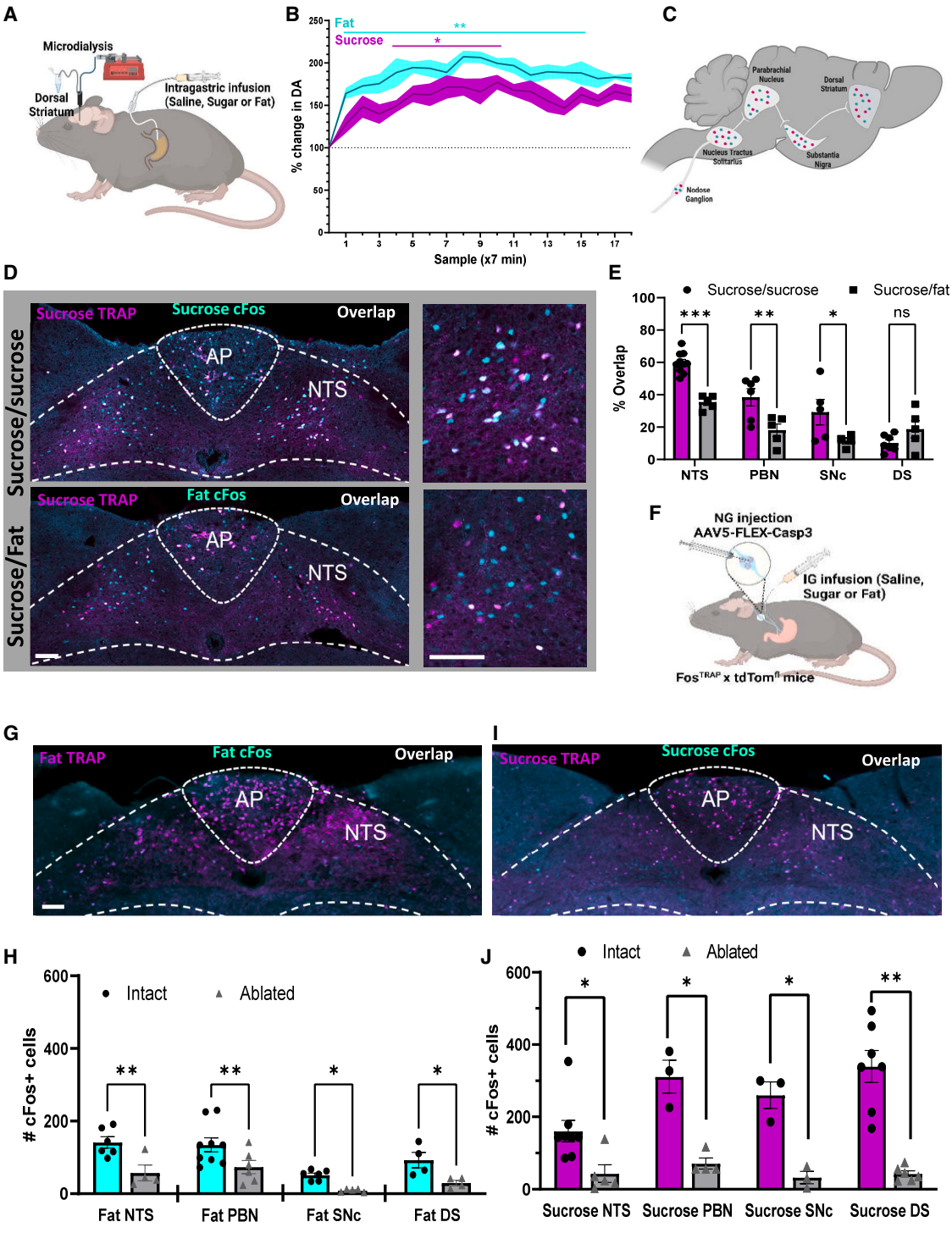

Figure 4. Fat and sugar recruit parallel but separate reward circuits

(A) Schematic illustrating microdialysis of the dorsal striatum performed to measure dopamine in response to 5 min of intragastric sucrose (15%) or fat (6.8%) compared with saline baseline.

(B) Rapid and sustained dopamine levels were found in response to both intragastric infusion of fat or sugar. n = 5. Two-way ANOVA with Holm-Sidak post hoc analysis.

(C) Schematic comparing neuronal activity in response to IG sucrose and IG fat along the gut-reward circuit.

(D) Representative images of the NTS in response to sucrose (TRAP, magenta), and colocalization after infusion 2 weeks later of sucrose (Fos, cyan; top) or fat (Fos, cyan; bottom) in the same animal. Higher magnification images on the right.

(legend continued on next page)

Please cite this article in press as: McDougle et al., Separate gut-brain circuits for fat and sugar reinforcement combine to promote overeating, Cell Metabolism (2023), https://doi.org/10.1016/j.cmet.2023.12.014

neurons (Figures S3H–S3J), highlighting that CCKaR is expressed in many different mechanosensory and chemosensory vagal sensory subpopulations[32] that innervate the length of the GI tract including the HPV.[31] Thus, CCKaR is a viable molecular marker of vagal sensory populations that sense both fat and sugar, but NG^{CCKaR} are a heterogeneous population that convey both sugar and fat reinforcement, but only fat and not sugar satiety.

Our results revealed vagal innervation of the HPV by Sugar^{TRAP} neurons. These data are consistent with previous work showing that the HPV receives nutrient-rich blood from multiple GI organs,[58] and vagal sensory innervation of the HPV wall is implicated in sensing of dietary glucose[59] and food preference.[60,61] To test the necessity of HPV-innervating vagal sensory neurons in post-ingestive reinforcement, we adapted a technique for targeting NG neurons based on their pattern of innervation (Figure 3G).[22] We first confirmed that a subset of left and right NG neurons[58,62] was labeled in response to brushing Cre-expressing retrograde adeno-associated virus (AAVrg-Cre) on the HPV wall of Ai14 mice (Figures 3H and S3K–S3M). Next, we selectively ablated HPV-innervating NG neurons by bilaterally injecting Cre-dependent caspase virus in the NG and applying AAVrg-Cre to the HPV wall of Ai14 mice (Figures 3G and 3H). In flavor-nutrient conditioning experiments, deletion of HPV-innervating NG neurons abolished sugar (Figure 3I), but not fat (Figure 3J), reinforcement. To assess the sufficiency of the hepatic branch of the vagus nerve in sugar reinforcement, we quantified Fos expression in the NTS in response to intragastric sucrose infusion in mice receiving sham, subdiaphragmatic vagotomy (SDV), or SDV while sparing the hepatic branch. Sucrose-induced NTS Fos expression was abolished by SDV but partially preserved in mice receiving SDV with spared hepatic branch (Figures 3K and 3L). Thus, we provide anatomical and behavioral data supporting a necessary role for HPV-innervating vagal sensory neurons in post-ingestive sugar reinforcement, and evidence that the hepatic vagal branch is partially sufficient to convey information about sugar to the brain. Altogether, these data indicate that sugar and fat reinforcement are mediated by separate vagal sensory populations that express CCKaR but can be distinguished based on their peripheral innervation patterns.

Separate central circuits for fat and sugar reinforcement

The vagus nerve acts as a key neural relay that connects the gut to dopamine-producing SNc neurons.[22] Optogenetic activation of gut-innervating vagal sensory neurons results in dopamine efflux in the DS and produces reward behaviors.[22] Thus, gut-innervating vagal sensory neurons are capable of mediating reinforcement to post-ingestive nutritive signals. Consistent with this notion, microdialysis sampling from the DS (Figure 4A) in mildly food-restricted awake mice results in rapid and sustained dopamine efflux in response to intragastric infusion of either fat (6.8% v/v) or sugar (15% w/v, Figure 4B).

Having demonstrated that fats and sugars are each capable of activating a nigrostriatal dopamine circuit, we inquired whether post-ingestive signals diverge at the cellular level along the well-defined gut-reward circuit[22] that comprises the NTS → dorsolateral parabrachial nucleus (dlPBN) → SNc → DS pathway (Figure 4C). We used Fos^{TRAP} mice to address the challenge of comparing neuronal activity in response to multiple stimuli at different time points over multiple brain regions in the same mouse. We validated the ability to compare Fos^{TRAP} neurons labeled with tdTomato and immunofluorescent (IF)-labeled Fos-expressing neurons following exposure to the same or different stimuli separated by 14 days in the same animal (Figures 4D and S4A–S4C). These findings support the concept that dissociable neuronal ensembles encode macronutrient-specific post-ingestive reinforcement. Based on previous studies,[27] we tested whether proenkephalin (*Penk*) could differentiate sugar- from fat-responsive neurons at the level of the NTS. *In situ* hybridization revealed that *Penk* was expressed in about a third of Sugar^{TRAP} and a quarter of Fat^{TRAP} NTS neurons (Figures S4L–S4Q).

When analyzing the overlap between sucrose^{TRAP} and sucrose Fos labeling, we found high overlap in the NTS, PBN, and SNc (Figure 4E). However, when comparing sucrose^{TRAP} and fat Fos labeling, there was only limited overlap between the neurons labeled during the two separate nutritive stimuli (Figure 4E). Interestingly, the overlap was reduced at more distal nodes of the gut-reward circuit, suggesting that some information is lost at each synapse but specificity is retained (Figures 4D and 4E). Notably, there was low overlap between Sugar^{TRAP} and sugar Fos in the DS, which may reflect the nature of dopamine signaling as discussed below in more detail. Together, these data indicate that fats and sugars recruit parallel and largely separate neuronal populations at each node of the gut-reward circuit, supporting the existence of distinguishable circuits for fat and sugar reinforcement.

We next addressed the necessity of nutrient-sensitive vagal sensory neurons in recruiting the nigrostriatal system. Within the same animal, we compared the neuronal activity along the gut-nigrostriatal circuit in response to a nutrient before and after

(E) Quantification showing higher overlap between repeated infusions of sucrose compared with separate macronutrients in the NTS, PBN, and SNc. n = 5–10. Two-way ANOVA with Holm-Sidak post hoc analysis.
(F) Schematic representing mice that received caspase-mediated ablation of NG neurons in response to intragastric infusion of nutrients to test the necessity of these neurons in recruiting fat or sugar specific gut-reward circuitry.
(G) Representative images of brain activity in response to fat was compared in the same mouse before (TRAP) and after (Fos) nutrient-induced ablation of NG neurons.
(H) Ablation of fat-sensing NG neurons blunts the response to subsequent response to fat at each level of the gut-reward circuit. Two-way ANOVA with Holm-Sidak post hoc analysis.
(I) Representative image of brain activity in response to sucrose was compared in the same mouse before (TRAP) and after (Fos) ablation of sucrose sensing NG neurons. n = 4–9.
(J) Ablation of sugar-sensing NG neurons blunts the response to subsequent response to sugar along the entire length of the gut-reward circuit. n = 3–8. Two-way ANOVA with Holm-Sidak post hoc analysis. Data are presented as mean ± SEM. *p < 0.05, **p < 0.01, ***p < 0.001, NS, not significant.

Please cite this article in press as: McDougle et al., Separate gut-brain circuits for fat and sugar reinforcement combine to promote overeating, Cell Metabolism (2023), https://doi.org/10.1016/j.cmet.2023.12.014

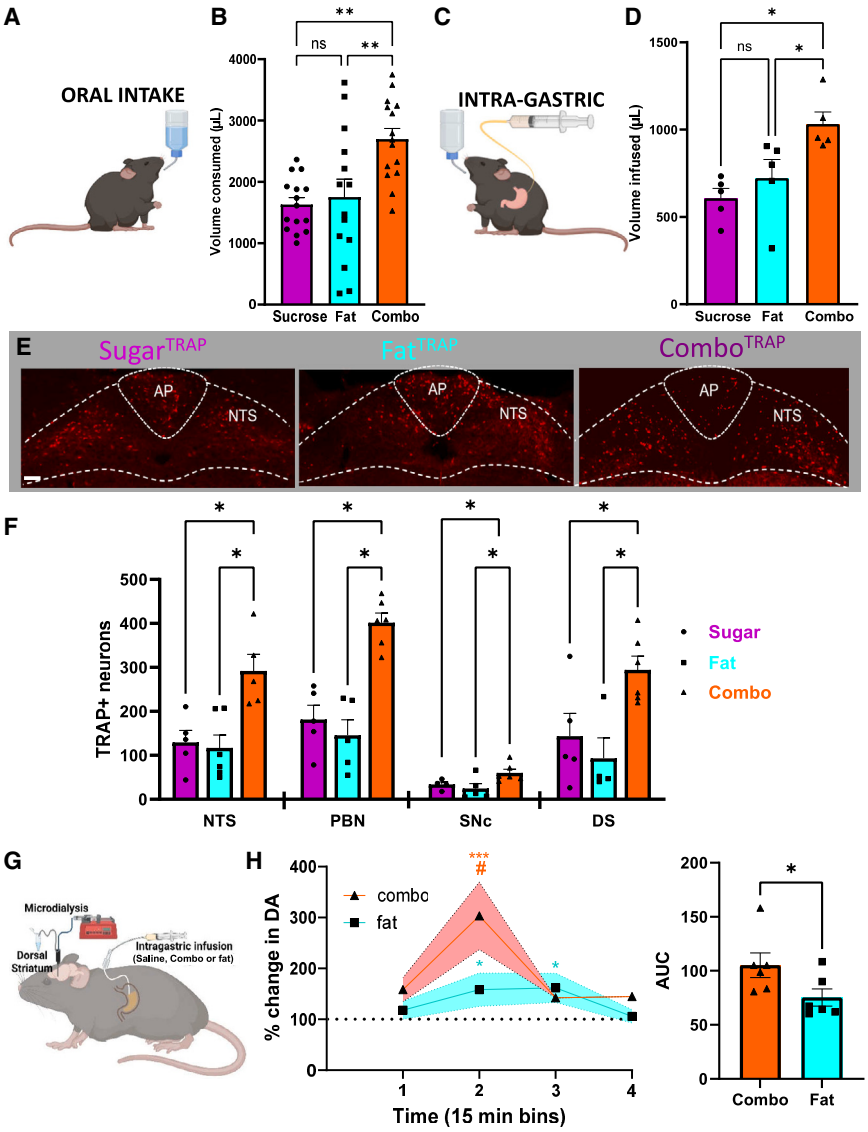

Figure 5. Combining fat and sugar additively increases intake and dopamine signaling

(A) Contact lickometer were used to measure mice voluntary intake of equicaloric solutions of fat, sugar or a mixture containing fat and sugar.

(B) Mice consumed larger volume of equicaloric combined solution than either fat or sugar alone in a one bottle licking test. n = 15. One-way ANOVA with Tukey post hoc analysis.

(C) Mice implanted with intragastric catheters licked non-nutritive flavored solutions for intragastric infusions of equicaloric solutions of sugar, fat or a solution containing both fat and sugar.

(D) Mice licked more to receive intragastric infusion of solution containing a combination of fat and sugar compared with equicaloric solutions of fat or sugar alone. n = 5. One-way ANOVA with Tukey post hoc analysis.

(E) Representative images of NTS.

(F) Quantification showing higher number of TRAP-labeled neurons in the NTS, PBN, SNc, and DS in response to solution containing the combination of fat and sugar compared with equicaloric solution of sugar or fat alone. Two-way ANOVA with Tukey post hoc analysis. *$p < 0.05$, **$p < 0.01$, ***$p < 0.001$.

(G) Schematic illustrating microdialysis of the dorsal striatum performed to measure dopamine in response to 5 min of intragastric fat (6.8%) or isocaloric combo (7.5% sucrose and 3.4% fat) compared with saline baseline.

(H) Higher dopamine levels were found in response to intragastric combo solution compared with fat. n = 6. Two-way ANOVA with Holm-Sidak post hoc analysis. *$p < 0.05$ from saline baseline and # represents $p < 0.05$ between combo and fat. Area under the curve (AUC) of dopamine over 1 h was significantly higher in response to combo solution compared with fat. n = 6 Wilcoxon signed rank test following confirmation that the AUC data were non-parametric. *$p < 0.05$. Data are presented as mean ± SEM.

deletion of vagal sensory neurons (Figure 4F). Cre-dependent caspase virus was bilaterally injected into the NG of Fos^{TRAP} mice, and neurons were trapped in response to intragastric infusion of sugar or fat with 4-OHT. This approach resulted in TRAP labeling with tdTomato in all responsive neurons (Figures S4D–S4K), whereas the caspase virus selectively ablated vagal sensory neurons that respond to the stimuli (Figures S4D–S4K). Robust tdTomato labeling was observed throughout the brain in response to both sugar (Figures S4D–S4G) and fat infusions (Figures S4H–S4K), indicating that the caspase virus had little impact on central processing of the initial post-ingestive signal. However, Fos IF was significantly blunted in the NTS (Figures 4G–4J and S4D–S4K), PBN (Figures 4H, 4J, and S4D–S4K), SNc (Figures 4H, 4J, and S4D–S4K), and DS (Figures 4H, 4J, and S4D–S4K) in response to individual macronutrients. These data suggest that nutrient interoception necessitates chemosensory vagal neurons to relay post-ingestive reinforcement for both fat and sugar to central dopamine circuits.

Combination of fat and sugar promotes overeating for pleasure

The implication of the above data is that combined activation of gut-reward circuits by sugar and fat may be more reinforcing and appetitive than either nutrient alone. To test this hypothesis, we quantified 30-min *ad libitum* intake in WT mice using a contact lickometer as mice voluntarily licked equicaloric solutions of fat, sucrose, or a mixture of the two macronutrients (Figure 5A). Mice readily consumed similar amounts of fat or sugar solutions, and strikingly, mice nearly doubled the number of licks for the solution containing a combination of fat and sugar compared with either fat or sugar alone (Figure 5B). We next assessed if mice show the same pattern of intake if the nutritive aspects of the solution are isolated from the oral component. Food-restricted WT mice with surgically implanted gastric catheters licked a non-nutritive flavored solution paired with intragastric infusions of equicaloric solutions of sugar, fat, or the combination (Figure 5C). After training, the mice exhibited an elevated licking pattern for

Please cite this article in press as: McDougle et al., Separate gut-brain circuits for fat and sugar reinforcement combine to promote overeating, Cell Metabolism (2023), https://doi.org/10.1016/j.cmet.2023.12.014

the mixed solution in this experimental paradigm (Figure 5D), suggesting that the increased preference for the combination of fat and sugar is independent of taste and is the result of post-ingestive signaling. Furthermore, intragastric infusion of a solution containing fat and sugar resulted in a supra-additive number of TRAP-labeled neurons in the NTS, PBN, SNc, and DS compared with animals TRAPed with equicaloric solutions of fat or sugar alone (Figures 5E, 5F, and S5). To determine if the combination of fat and sugar causes higher levels of dopamine release compared with isocaloric solution of a single macronutrient, we performed microdialysis in the DS in response to intragastric infusion (Figure 5G). We found that intragastric infusion of both fat and combo increased dopamine compared with baseline (Figure 5H). However, in the first 30 min, intragastric infusion of the combo solution resulted in higher dopamine release in the DS compared with equicaloric fat infusion (Figure 5H). These data provide additional support that there are separable circuits for fat and sugar reinforcement and suggest that foods rich in both fats and sugars combine to additively recruit both sugar and fat reward circuits, promoting higher levels of motivation to consume obesogenic diets.

DISCUSSION

Our findings reveal the existence of separable circuits for sugar and fat reinforcement. Using *in vivo* calcium imaging of NG, we first identified two vagal sensory populations that respond separately to post-ingestive fats or sugars. We then employ a Fos^{TRAP} approach to delineate the anatomy and function of these neurons. We reveal that these two distinct vagal populations (1) innervate separate peripheral organs, (2) are necessary for nutrient-specific reinforcement, and (3) initiate parallel gut-brain reward circuits that can be dissociated at the cellular level. The activation of separate fat or sugar circuits can increase motivated feeding behavior, but strikingly, the combination of fats and sugars synergize to supra-additively increase the activity of neurons along the gut-reward circuit, increase dopamine release, and promote overeating independently of calories. Thus, we describe a novel mechanism involving parallel activation of food reward circuits to transmit the internal drive to consume obesogenic foods.

Identifying the function of chemosensory NG neurons

Our data identify a novel role of chemosensory NG populations in signaling nutrient reinforcement. The NG is composed of heterogeneous populations of vagal neurons responsive to various sensory modalities. Two populations of tension-sensitive mechanosensory NG neurons have been identified that form either intramuscular arrays in the muscle layers or intraganglionic laminar endings in the myenteric plexis.[34,63] A separate chemosensory NG population was identified in the 1950s[64] based on electrophysiological responses to chemical, but not mechanical, stimuli.[64–66] Tracing experiments supported that these chemosensory NG neurons form distinct mucosal endings in intestinal villi,[31] suggesting that they were ideally situated to respond to absorbed nutrients and hormone products from the gut epithelium. Transcriptomic sequencing of NG later confirmed that chemosensory populations are genetically distinct from mechanosensory neurons.[31] Although optogenetic stimulation of genetically defined mechanoreceptors potently inhibited acute food intake, stimulation of chemosensory neurons did not[31]; thus, the function of chemosensory neurons has remained elusive. Here, we used a Fos^{TRAP} approach to functionally target a population of NG neurons that are nutrient-sensitive, and we demonstrate that these neurons form mucosal terminals in intestinal villi—a hallmark of chemosensory neurons. Using viral-mediated ablation and optogenetic stimulation approaches, we demonstrate that these chemosensory neurons engage gut-brain reward circuits and cause nutrient-specific reinforcement and appetition for food. Several prior studies using less precise tools, including resection of subdiaphragmatic vagus nerve while sparing the hepatic branch, have resulted in variable outcomes, ranging from completely abolishing the preference to the carbohydrate polycose in an hour preference test to no effect in a 24-h preference test in the same animals.[67] Here, we find that complete SDV abolishes Fos activity in the NTS in response to intragastric infusion of sugar but that this is partially rescued by sparing the hepatic branch of the vagus nerve, suggesting that the site of the resection is an important factor. Notably, these types of experiments are difficult to interpret because of the confound caused by the deletion of vagal motor signaling that controls gut function. This issue is partially addressed by chemically induced vagal deafferentation using capsaicin.[68] Capsaicin experiments also show no impairment of fat or sugar reinforcement[28]; however, capsaicin causes cell death by acting at TRPV1 channels, which are not expressed in many NG neurons that are assumed to be chemosensory populations based on transcriptomic analysis.[32] This suggests that capsaicin treatment may spare key vagal sensory neurons required for fat and sugar reinforcement. Importantly, more selective approaches that do not impair motor control of gut function support a role for the gut-brain axis in relaying food reward.[22,27,69]

Using a Fos^{TRAP} strategy that enables the most nutrient-specific vagal deafferentation to date, we demonstrate that separate vagal circuits convey sugar or fat reinforcement. We provide multiple lines of evidence that Fos^{TRAP} is an effective strategy that provides permanent genetic access to vagal sensory neuron populations based on their response to defined sensory stimuli, unbiased by genetically defined cell type. First, using calcium imaging, we confirm that Sugar^{TRAP} NG neurons are activated in response to intraduodenal infusion of sugar, but not fat. Second, we demonstrate that caspase-mediated ablation of nutrient-responsive NG neurons prevents nutrient-specific reinforcement. Third, we show that ablation of a nutrient-specific vagal circuit impairs downstream neural activity in the nigrostriatal dopamine pathway. Furthermore, we find that tracing from Fat^{TRAP} and Sugar^{TRAP} results in different GI innervation patterns. Finally, we confirm that post-ingestive sugar reinforcement requires vagal sensory neurons that innervate the HPV. These data support prior work predicting genetic heterogeneity based on sensory modality[32] but suggest a previously unsuspected amount of cellular diversification according to sensitivity to individual luminal nutritive stimuli. Thus, we provide direct evidence that chemosensory neurons play a key role in food choice and ensure the consumption of nutritive foods.

Fat- and sugar-sensing vagal neurons can be differentiated based on their innervation of the HPV. The portal vein is known to receive dietary sugar from the intestine and subjected to

Please cite this article in press as: McDougle et al., Separate gut-brain circuits for fat and sugar reinforcement combine to promote overeating, Cell Metabolism (2023), https://doi.org/10.1016/j.cmet.2023.12.014

wide fluctuations in glucose concentrations between fed and fasted conditions.[70] Portal vein sensing of sugar reduces food intake[71–74] and plays a critical role in maintaining blood glucose levels.[75–77] Although the HPV signals to the brain via both spinal and vagal afferent pathways,[58] only the spinal pathway is necessary for HPV-mediated sugar satiety[78] by inhibiting activity of hunger neurons in the hypothalamus (ARC^{AgRP})[57] and the counterregulatory response to hypoglycemia.[59,79] Thus, the physiological role of vagal neurons that respond to HPV infusions of sugar[80] remained poorly defined. In this study, we report that the vagal innervation of the HPV is sufficient to convey at least part of intragastric sugar signaling to the NTS and necessary for sucrose reinforcement.

The molecular markers that delineate fat- and sugar-sensing vagal sensory neurons remain poorly defined. Both types of neuronal populations express CCK receptors and these NG^{Cckar} neurons are necessary for both sugar and fat reinforcement. The lack of specificity of CCK receptor as a marker for sugar or fat sensing by vagal sensory neurons is not surprising, given the abundance of CCKaR expressing neurons in the NG as shown here and by others,[81] a conclusion that is further supported by evidence that CCK receptor expressing NG neurons are responsive to both intragastric infusion of fat or sugar.[82] Given the prevalence of these NG^{Cckar} neurons, it is unsurprising that they may comprise heterogeneous populations that convey diverse information about a meal that can result in a range of feeding behaviors. In addition to their role in fat and sugar reinforcement, we report that NG^{Cckar} neurons are involved in fat satiety, confirming previous work in rats showing that deletion of these neurons has no effect on chow intake but significantly increases food intake and body weight in response to a high fat diet.[56] As discussed above, fat- and sugar-sensitive vagal neuron populations can be further subcategorized based on their innervation of the HPV. Prior vagal sensory neuron-sequencing data identified multiple clusters of *Cckar* neurons, including a chemosensory cluster t6[31] or G[32] characterized by co-expression of *Vip*, *Htr3a*, and *Ust2b*, and a separate polymodal cluster t3/t1[31] or I[32] that co-express *Oxtr*, *Car8*, and *Ctnx2*. Both of these clusters respond to luminal glucose infusion[32] and a fraction of neurons in each of these clusters innervate the HPV and the duodenum.[31] Therefore, these may be viable candidate markers of sugar-sensitive vagal populations. Another large population of chemosensory neurons characterized by *Gpr65* expression were identified in cluster t9-12[31] and F.[32] The role of NG^{Gpr65} neurons as fat and/or sugar sensors remains unclear because (1) they do not appear to co-express *Cckar* and (2) prior work suggests that they exhibit broad response to intestinal stimuli,[33] consistent with a role as polymodal osmosensors.[83] TRPA1 has recently been reported to be a marker of fat-responsive vagal sensory neurons.[82] However, NG^{Trpa1} neurons are sensitive to mechanosensory stimuli[32]; thus, additional work is required to determine whether neural activity of TRPA1 neurons to fat is a consequence of fat sensing per se rather than fat-induced intestinal stretch. Another issue is that TRPA1 neurons innervate the lungs,[32] suggesting that this marker is not specific to a vagal population responsible for intestinally derived fat reinforcement. Thus, fat and sugar NG neurons may be composed of genetically heterogeneous populations, and it remains unclear whether they can be delineated on the basis of a single genetic marker. An advantage of the Fos^{TRAP} approach is that it circumvents the need for *a priori* knowledge of genetic markers and innervation patterns. Using this approach, we demonstrate that separate NG populations sense intestinal nutrients and drive nutrient-specific reinforcement. This strategy could therefore be employed in future to gain a comprehensive understanding of neurons responsive to nutrients, hormones, microbial metabolites, and inflammatory signals in gut-brain control of physiological processes and motivated behavior across health and disease states.

Integration of post-ingestive reinforcement by nigrostriatal circuits

Motivated behavior is driven by the ability to derive value from the outcome of an action. The nigrostriatal circuit, whereby SNc neurons release dopamine onto DS neurons, is essential for modulating acquisition and updating motivated behaviors,[84,85] including the motivation to eat.[21] We and others have demonstrated that the presence of nutrients in the gut evokes dopamine release in the DS. Importantly, the amount of dopamine efflux correlates with caloric load,[18,86] and inhibition of dopamine signaling in the DS increases food intake, suggesting that increased dopamine release drives motivation to eat.[22] In human neuroimaging studies, striatal activity similarly increased in response to food images.[87] The use of fMRI and positron emission tomography methodology demonstrates that the delayed post-ingestive response to food intake modulated dopamine signaling within the nigrostriatal circuit.[19] Notably, pharmacological interventions that reduce dopaminergic tone have provided evidence for lower effort spending and motivation in both rodents[22,88] and humans.[89,90] We establish that separate nutrient-derived gut-brain circuits input into the nigrostriatal system to establish distinct motivation for fat or sugar. Importantly, foods that combine fats and sugars simultaneously engage these two separable gut-brain circuits to increase dopamine release and reinforce the choice to select and consume these obesogenic foods.

Interestingly, we observed that the level of overlap in response to repeated infusion of the same nutrient reduced along the length of the gut-reward circuit, with very low overlap observed in the DS. This finding was consistent across animals irrespective of the nutrient. The mechanisms for this are unclear but may reflect the variable response of neurons to repeated identical stimuli.[91] In response to a physiological stimulus such as nutrient sensing in the gut, the probability of a neuron firing will be highest in the sensory neurons and reduce at more distal nodes of the circuit. In addition, the extremely low overlap in DS activity may be specific to dopamine signaling. Neuromodulators, such as dopamine, are typically released by volume transmission and diffuse to activate receptors on numerous target cells, exerting widespread effects.[92] Although *ex vivo* studies indicate that dopamine can directly activate certain types of spiny projection neurons (dSPNs) and inhibit others (iSPNs), it is believed that its effects *in vivo* are more intricate. This is because dopamine receptors are not only present on the targeted neurons (SPNs) but also on other components of the brain circuitry, including excitatory afferents, SPNs inhibitory collaterals, and interneurons in the striatum. These various elements collectively shape the output of the striatum.[93] Recent *in vivo* calcium imaging

Please cite this article in press as: McDougle et al., Separate gut-brain circuits for fat and sugar reinforcement combine to promote overeating, Cell Metabolism (2023), https://doi.org/10.1016/j.cmet.2023.12.014

study from the striatum of behaving mice aligns with the previously described sparsity of the sensorimotor code in the DS.[94,95] Specifically, only 10% of the total active group in the DS were activated in response to each *in vivo* stimulus. It was observed that individual dSPNs and iSPNs did not consistently exhibit activity during different instances of behavior. Furthermore, the size of the activated groups remained similar over time, whether the imaging was conducted a few days or a month apart.[96] Thus, the limited colocalization of Fos in response to repeated infusion of the same nutrient in the current study may reflect intrinsic properties of this dopaminergic circuit.

Foods rich in fat and sugar are rarely found in nature.[97,98] Thus, prior to the development of industrialized farming in our recent past, the ability to locate foods with different energy sources would have provided a competitive advantage to evolve macronutrient-distinct circuits for dopamine-mediated learning and motivation. The modern food environment has led to the development of processed foods that incorporate high levels of fats and sugars.[99] It has been previously demonstrated that human subjects want foods that combine fat and carbohydrate more than foods that contain fat or carbohydrate alone, and this correlated with supra-additive striatal responses.[98] Our results expand this prior work by identifying a neural mechanism to explain why the combination of fat and sugar is more rewarding than either alone. We find that mice voluntarily increase oral or intragastric intake of calorie-matched solutions and increase dopamine release in response to the combination of both fats and sugars compared with single macronutrients, suggesting that motivated feeding behavior occurs by post-ingestive signals independently of oral stimuli. These data are consistent with preference for oral stimuli (e.g., flavor, texture, and taste) being a conditioned response that predicts post-ingestive reward. This mechanism likely reflects a conserved system that evolved in rodents and humans to convey separate interoceptive information about the source of energy to the brain and could suggest the existence of "labeled lines" or hardwired pathways for fat and sugar reinforcement. In our current food environment, readily available foods rich in both fats and sugars, thus, result in greater valuation and appetition of obesogenic diets and may therefore increase the predisposition to the development of obesity.

Conclusions

Our data support the idea that increased caloric intake of Western diet results from hijacking interoceptive circuits that separately reinforce fats and sugars. Because interoceptive signaling occurs below the level of consciousness, the motivation to consume obesogenic diets may occur without cognitive perception.[100] In other words, conscious dieting efforts may be overpowered by the subconscious internal drive to consume foods rich in both fats and sugars. Therefore, manipulating interoceptive gut-reward circuits may provide a viable therapeutic target for treating obesity by promoting voluntary reduction in the consumption of obesogenic diets.

Limitations of the study

In this study, we employed the TRAP2 genetic mouse model to investigate gut-brain circuits for sugar and fat reinforcement. Limitations of this approach are that it relies on the *Fos* promoter; thus, only neurons that are activated in response to a stimulus were targeted. Taking this into account, it remains challenging to determine the extent to which neurons with high constitutive activity or that do not express Fos are involved in fat and sugar reinforcement. This is not a major issue when studying vagal sensory neurons that are almost exclusively glutamatergic; however, additional single-cell resolution *in vivo* approaches will need to be employed to fully elucidate the complexity of central neural circuits for reinforcement of distinct nutrients.

STAR★METHODS

Detailed methods are provided in the online version of this paper and include the following:

- KEY RESOURCES TABLE
- RESOURCE AVAILABILITY
  - Lead contact
  - Materials availability
  - Data and code availability
- EXPERIMENTAL MODEL DETAILS
  - Animals
- METHOD DETAILS
  - TRAP protocol
  - Surgeries
  - Behavioral Tests
  - Tissue processing & storage
- QUANTIFICATION AND STATISTICAL ANALYSIS

SUPPLEMENTAL INFORMATION

Supplemental information can be found online at https://doi.org/10.1016/j.cmet.2023.12.014.

ACKNOWLEDGMENTS

This study was supported by NIH grants R01 DK116004 (G.d.L.), R01 DK094871 (G.d.L.), F31 DK1311773 (M.M.), start-up funds (G.d.L. and A. Sharma), AHA postdoctoral fellowship 23POST1026084 (A. Singh), F32 DK128984 (L.N.W.), and grants from SanteDige foundation and Phillip foundation (V.P.). The images used for graphical abstract and in Figures 1A, 1G, 2A, 2E, 2I, 3A, 3D, 3G, 4A, 4C, 4F, 5A, 5C, S3A, and S3K were created using BioRender.com. We thank M. Afaghani at the University of Florida for technical assistance collecting pilot data and acknowledge A. Alhadeff, M.A. Lazar, and J. de Lartigue for constructive comments on the manuscript.

AUTHOR CONTRIBUTIONS

Conceptualization, G.d.L. and M.M.; methodology, G.d.L., M.M., N.U., and A. Sharma; investigation, M.M., A.d.A., A. Singh, M.Y., I.B., V.P., R.M.-H., M.V., L.N.W., and A.G.; writing – original draft, G.d.L.; writing – review and editing, all authors; funding acquisition, G.d.L., M.M., A. Singh, and A. Sharma; resources, G.L., A. Sharma, N.U., and B.W.; project administration, G.L.; and supervision, G.L. and A. Sharma.

DECLARATION OF INTERESTS

The authors declare no competing interests.

INCLUSION AND DIVERSITY

We support inclusive, diverse, and equitable conduct of research.

Please cite this article in press as: McDougle et al., Separate gut-brain circuits for fat and sugar reinforcement combine to promote overeating, Cell Metabolism (2023), https://doi.org/10.1016/j.cmet.2023.12.014

Received: February 2, 2023
Revised: September 25, 2023
Accepted: December 11, 2023
Published: January 18, 2024

REFERENCES

1. Hall, K.D. (2018). Did the food environment cause the obesity epidemic? Obesity (Silver Spring) *26*, 11–13.
2. Berthoud, H.R., Morrison, C.D., Ackroff, K., and Sclafani, A. (2021). Learning of food preferences: mechanisms and implications for obesity & metabolic diseases. Int. J. Obes. (Lond) *45*, 2156–2168.
3. Glendinning, J.I., Gillman, J., Zamer, H., Margolskee, R.F., and Sclafani, A. (2012). The role of T1r3 and Trpm5 in carbohydrate-induced obesity in mice. Physiol. Behav. *107*, 50–58.
4. Larsson, M.H., Håkansson, P., Jansen, F.P., Magnell, K., and Brodin, P. (2015). Ablation of TRPM5 in mice results in reduced body weight gain and improved glucose tolerance and protects from excessive consumption of sweet palatable food when fed high caloric diets. PLOS One *10*, e0138373.
5. Ferreira, J.G., Tellez, L.A., Ren, X., Yeckel, C.W., and de Araujo, I.E. (2012). Regulation of fat intake in the absence of flavour signalling. J. Physiol. *590*, 953–972.
6. Tordoff, M.G., Pearson, J.A., Ellis, H.T., and Poole, R.L. (2017). Does eating good-tasting food influence body weight? Physiol. Behav. *170*, 27–31.
7. Holman, G.L. (1969). Intragastric reinforcement effect. J. Comp. Physiol. Psychol. *69*, 432–441.
8. Baker, B.J., Booth, D.A., Duggan, J.P., and Gibson, E.L. (1987). Protein appetite demonstrated: learned specificity of protein-cue preference to protein need in adult rats. Nutr. Res. *7*, 481–487.
9. Sherman, J.E., Hickis, C.F., Rice, A.G., Rusiniak, K.W., and Garcia, J. (1983). Preferences and aversions for stimuli paired with ethanol in hungry rats. Anim. Learn. Behav. *11*, 101–106.
10. Sclafani, A., and Nissenbaum, J.W. (1988). Robust conditioned flavor preference produced by intragastric starch infusions in rats. Am. J. Physiol. *255*, R672–R675.
11. de Araujo, I.E. (2016). Circuit organization of sugar reinforcement. Physiol. Behav. *164*, 473–477.
12. Sclafani, A. (2001). Post-ingestive positive controls of ingestive behavior. Appetite *36*, 79–83.
13. Sclafani, A., and Glendinning, J.I. (2005). Sugar and fat conditioned flavor preferences in C57BL/6J and 129 mice: oral and postoral interactions. Am. J. Physiol. Regul. Integr. Comp. Physiol. *289*, R712–R720.
14. Ramirez, I. (1994). Stimulation of fluid intake by carbohydrates: interaction between taste and calories. Am. J. Physiol. *266*, R682–R687.
15. Ludwig, D.S., Aronne, L.J., Astrup, A., de Cabo, R., Cantley, L.C., Friedman, M.I., Heymsfield, S.B., Johnson, J.D., King, J.C., Krauss, R.M., et al. (2021). The carbohydrate-insulin model: a physiological perspective on the obesity pandemic. Am. J. Clin. Nutr. *114*, 1873–1885.
16. Drewnowski, A. (2007). The real contribution of added sugars and fats to obesity. Epidemiol. Rev. *29*, 160–171.
17. Brayner, B., Kaur, G., Keske, M.A., Perez-Cornago, A., Piernas, C., and Livingstone, K.M. (2021). Dietary patterns characterized by fat type in association with obesity and Type 2 diabetes: A longitudinal study of UK Biobank participants. J. Nutr. *151*, 3570–3578.
18. Tellez, L.A., Han, W., Zhang, X., Ferreira, T.L., Perez, I.O., Shammah-Lagnado, S.J., van den Pol, A.N., and de Araujo, I.E. (2016). Separate circuitries encode the hedonic and nutritional values of sugar. Nat. Neurosci. *19*, 465–470.
19. Thanarajah, S.E., Backes, H., DiFeliceantonio, A.G., Albus, K., Cremer, A.L., Hanssen, R., Lippert, R.N., Cornely, O.A., Small, D.M., Brüning, J.C., et al. (2019). Food intake recruits orosensory and post-ingestive dopaminergic circuits to affect eating desire in humans. Cell Metab. *29*, 695–706.e4.
20. Szczypka, M.S., Kwok, K., Brot, M.D., Marck, B.T., Matsumoto, A.M., Donahue, B.A., and Palmiter, R.D. (2001). Dopamine production in the caudate putamen restores feeding in dopamine-deficient mice. Neuron *30*, 819–828.
21. Palmiter, R.D. (2008). Dopamine signaling in the dorsal striatum is essential for motivated behaviors: lessons from dopamine-deficient mice. Ann. N. Y. Acad. Sci. *1129*, 35–46.
22. Han, W., Tellez, L.A., Perkins, M.H., Perez, I.O., Qu, T., Ferreira, J., Ferreira, T.L., Quinn, D., Liu, Z.W., Gao, X.B., et al. (2018). A neural circuit for gut-induced reward. Cell *175*, 665–678.e23.
23. Randich, A., Tyler, W.J., Cox, J.E., Meller, S.T., Kelm, G.R., and Bharaj, S.S. (2000). Responses of celiac and cervical vagal afferents to infusions of lipids in the jejunum or ileum of the rat. Am. J. Physiol. Regul. Integr. Comp. Physiol. *278*, R34–R43.
24. Mei, N. (1978). Vagal glucoreceptors in the small intestine of the cat. J. Physiol. *282*, 485–506.
25. Tellez, L.A., Medina, S., Han, W., Ferreira, J.G., Licona-Limón, P., Ren, X., Lam, T.T., Schwartz, G.J., and de Araujo, I.E. (2013). A gut lipid messenger links excess dietary fat to dopamine deficiency. Science *341*, 800–802.
26. Han, W., Tellez, L.A., Niu, J., Medina, S., Ferreira, T.L., Zhang, X., Su, J., Tong, J., Schwartz, G.J., van den Pol, A., and de Araujo, I.E. (2016). Striatal dopamine links gastrointestinal rerouting to altered sweet appetite. Cell Metab. *23*, 103–112.
27. Tan, H.-E., Sisti, A.C., Jin, H., Vignovich, M., Villavicencio, M., Tsang, K.S., Goffer, Y., and Zuker, C.S. (2020). The gut–brain axis mediates sugar preference. Nature *580*, 511–516.
28. Sclafani, A., and Ackroff, K. (2019). Capsaicin-induced visceral deafferentation does not attenuate flavor conditioning by intragastric fat infusions in mice. Physiol. Behav. *208*, 112586.
29. Sclafani, A., Ackroff, K., and Schwartz, G.J. (2003). Selective effects of vagal deafferentation and celiac-superior mesenteric ganglionectomy on the reinforcing and satiating action of intestinal nutrients. Physiol. Behav. *78*, 285–294.
30. Sclafani, A., and Kramer, T.H. (1983). Dietary selection in vagotomized rats. J. Auton. Nerv. Syst. *9*, 247–258.
31. Bai, L., Mesgarzadeh, S., Ramesh, K.S., Huey, E.L., Liu, Y., Gray, L.A., Aitken, T.J., Chen, Y., Beutler, L.R., Ahn, J.S., et al. (2019). Genetic identification of vagal sensory neurons that control feeding. Cell *179*, 1129–1143.e23.
32. Zhao, Q., Yu, C.D., Wang, R., Xu, Q.J., Dai Pra, R., Zhang, L., and Chang, R.B. (2022). A multidimensional coding architecture of the vagal interoceptive system. Nature *603*, 878–884.
33. Williams, E.K., Chang, R.B., Strochlic, D.E., Umans, B.D., Lowell, B.B., and Liberles, S.D. (2016). Sensory neurons that detect stretch and nutrients in the digestive system. Cell *166*, 209–221.
34. Berthoud, H.-R., and Neuhuber, W.L. (2000). Functional and chemical anatomy of the afferent vagal system. Auton. Neurosci. *85*, 1–17.
35. Prescott, S.L., and Liberles, S.D. (2022). Internal senses of the vagus nerve. Neuron *110*, 579–599.
36. Makhmutova, M., Weitz, J., Tamayo, A., Pereira, E., Boulina, M., Almaça, J., Rodriguez-Diaz, R., and Caicedo, A. (2021). Pancreatic β-cells communicate with vagal sensory neurons. Gastroenterology *160*, 875–888.e11.
37. Madisen, L., Garner, A.R., Shimaoka, D., Chuong, A.S., Klapoetke, N.C., Li, L., van der Bourg, A., Niino, Y., Egolf, L., Monetti, C., et al. (2015). Transgenic mice for intersectional targeting of neural sensors and effectors with high specificity and performance. Neuron *85*, 942–958.
38. Gentilcore, D., Chaikomin, R., Jones, K.L., Russo, A., Feinle-Bisset, C., Wishart, J.M., Rayner, C.K., and Horowitz, M. (2006). Effects of fat on gastric emptying of and the glycemic, insulin, and incretin responses to

Please cite this article in press as: McDougle et al., Separate gut-brain circuits for fat and sugar reinforcement combine to promote overeating, Cell Metabolism (2023), https://doi.org/10.1016/j.cmet.2023.12.014

a carbohydrate meal in Type 2 diabetes. J. Clin. Endocrinol. Metab. *91*, 2062–2067.

39. McHugh, P.R., and Moran, T.H. (1979). Calories and gastric emptying: a regulatory capacity with implications for feeding. Am. J. Physiol. *236*, R254–R260.
40. Roura, E., Depoortere, I., and Navarro, M. (2019). Review: chemosensing of nutrients and non-nutrients in the human and porcine gastrointestinal tract. Animal *13*, 2714–2726.
41. DeNardo, L.A., Liu, C.D., Allen, W.E., Adams, E.L., Friedmann, D., Fu, L., Guenthner, C.J., Tessier-Lavigne, M., and Luo, L. (2019). Temporal evolution of cortical ensembles promoting remote memory retrieval. Nat. Neurosci. *22*, 460–469.
42. Guenthner, C.J., Miyamichi, K., Yang, H.H., Heller, H.C., and Luo, L. (2013). Permanent genetic access to transiently active neurons via TRAP: targeted recombination in active populations. Neuron *78*, 773–784.
43. Pool, A.H., Wang, T., Stafford, D.A., Chance, R.K., Lee, S., Ngai, J., and Oka, Y. (2020). The cellular basis of distinct thirst modalities. Nature *588*, 112–117.
44. Allen, W.E., DeNardo, L.A., Chen, M.Z., Liu, C.D., Loh, K.M., Fenno, L.E., Ramakrishnan, C., Deisseroth, K., and Luo, L. (2017). Thirst-associated preoptic neurons encode an aversive motivational drive. Science *357*, 1149–1155.
45. Madisen, L., Zwingman, T.A., Sunkin, S.M., Oh, S.W., Zariwala, H.A., Gu, H., Ng, L.L., Palmiter, R.D., Hawrylycz, M.J., Jones, A.R., et al. (2010). A robust and high-throughput Cre reporting and characterization system for the whole mouse brain. Nat. Neurosci. *13*, 133–140.
46. Lo, C.-M., Ma, L., Zhang, D.M., Lee, R., Qin, A., Liu, M., Woods, S.C., Sakai, R.R., Raybould, H.E., and Tso, P. (2007). Mechanism of the induction of brain c-Fos-positive neurons by lipid absorption. Am. J. Physiol. Regul. Integr. Comp. Physiol. *292*, R268–R273.
47. Yamamoto, T., and Sawa, K. (2000). c-Fos-like immunoreactivity in the brainstem following gastric loads of various chemical solutions in rats. Brain Res. *866*, 135–143.
48. Streefland, C., Farkas, E., Maes, F.W., and Bohus, B. (1996). C-fos expression in the brainstem after voluntary ingestion of sucrose in the rat. Neurobiology (Bp) *4*, 85–102.
49. Rogers, R.C., and Hermann, G.E. (2008). Mechanisms of action of CCK to activate central vagal afferent terminals. Peptides *29*, 1716–1725.
50. Yang, C.F., Chiang, M.C., Gray, D.C., Prabhakaran, M., Alvarado, M., Juntti, S.A., Unger, E.K., Wells, J.A., and Shah, N.M. (2013). Sexually dimorphic neurons in the ventromedial hypothalamus govern mating in both sexes and aggression in males. Cell *153*, 896–909.
51. Madisen, L., Mao, T., Koch, H., Zhuo, J.M., Berenyi, A., Fujisawa, S., Hsu, Y.W., Garcia, A.J., 3rd, Gu, X., Zanella, S., et al. (2012). A toolbox of Cre-dependent optogenetic transgenic mice for light-induced activation and silencing. Nat. Neurosci. *15*, 793–802.
52. Brierley, D.I., Holt, M.K., Singh, A., de Araujo, A., McDougle, M., Vergara, M., Afaghani, M.H., Lee, S.J., Scott, K., Maske, C., et al. (2021). Central and peripheral GLP-1 systems independently suppress eating. Nat. Metab. *3*, 258–273.
53. Olds, J. (1976). Do reward and drive neurons exist? In Psychopathology of Human Adaptation, G. Serban, ed. (Springer), pp. 47–75.
54. Olds, J., and Milner, P. (1954). Positive reinforcement produced by electrical stimulation of septal area and other regions of rat brain. J. Comp. Physiol. Psychol. *47*, 419–427.
55. Diepenbroek, C., Quinn, D., Stephens, R., Zollinger, B., Anderson, S., Pan, A., and de Lartigue, G. (2017). Validation and characterization of a novel method for selective vagal deafferentation of the gut. Am. J. Physiol. Gastrointest. Liver Physiol. *313*, G342–G352.
56. McDougle, M., Quinn, D., Diepenbroek, C., Singh, A., de la Serre, C., and de Lartigue, G. (2021). Intact vagal gut-brain signalling prevents hyperphagia and excessive weight gain in response to high-fat high-sugar diet. Acta Physiol. Oxf. *231*, e13530.
57. Goldstein, N., McKnight, A.D., Carty, J.R.E., Arnold, M., Betley, J.N., and Alhadeff, A.L. (2021). Hypothalamic detection of macronutrients via multiple gut-brain pathways. Cell Metab. *33*, 676–687.e5.
58. Garcia-Luna, C., Sanchez-Watts, G., Arnold, M., de Lartigue, G., DeWalt, N., Langhans, W., and Watts, A.G. (2021). The medullary targets of neurally conveyed sensory information from the rat hepatic portal and superior mesenteric veins. eNeuro *8*, 0419–0420.2021.
59. Mithieux, G., Misery, P., Magnan, C., Pillot, B., Gautier-Stein, A., Bernard, C., Rajas, F., and Zitoun, C. (2005). Portal sensing of intestinal gluconeogenesis is a mechanistic link in the diminution of food intake induced by diet protein. Cell Metab. *2*, 321–329.
60. Zhang, L., Han, W., Lin, C., Li, F., and de Araujo, I.E. (2018). Sugar metabolism regulates flavor preferences and portal glucose sensing. Front. Integr. Neurosci. *12*, 57.
61. Delaere, F., Akaoka, H., De Vadder, F., Duchampt, A., and Mithieux, G. (2013). Portal glucose influences the sensory, cortical and reward systems in rats. Eur. J. Neurosci. *38*, 3476–3486.
62. Teratani, T., Mikami, Y., Nakamoto, N., Suzuki, T., Harada, Y., Okabayashi, K., Hagihara, Y., Taniki, N., Kohno, K., Shibata, S., et al. (2020). The liver-brain-gut neural arc maintains the T(reg) cell niche in the gut. Nature *585*, 591–596.
63. Brookes, S.J.H., Spencer, N.J., Costa, M., and Zagorodnyuk, V.P. (2013). Extrinsic primary afferent signalling in the gut. Nat. Rev. Gastroenterol. Hepatol. *10*, 286–296.
64. Paintal, A.S. (1957). Responses from mucosal mechanoreceptors in the small intestine of the cat. J. Physiol. *139*, 353–368.
65. Clarke, G.D., and Davison, J.S. (1978). Mucosal receptors in the gastric antrum and small intestine of the rat with afferent fibres in the cervical vagus. J. Physiol. *284*, 55–67.
66. Leek, B.F. (1977). Abdominal and pelvic visceral receptors. Br. Med. Bull. *33*, 163–168.
67. Sclafani, A., and Lucas, F. (1996). Abdominal vagotomy does not block carbohydrate-conditioned flavor preferences in rats. Physiol. Behav. *60*, 447–453.
68. Browning, K.N., Babic, T., Holmes, G.M., Swartz, E., and Travagli, R.A. (2013). A critical re-evaluation of the specificity of action of perivagal capsaicin. J. Physiol. *591*, 1563–1580.
69. Kaelberer, M.M., Buchanan, K.L., Klein, M.E., Barth, B.B., Montoya, M.M., Shen, X., and Bohórquez, D.V. (2018). A gut-brain neural circuit for nutrient sensory transduction. Science *361*, eaat5236.
70. Strubbe, J.H., and Steffens, A.B. (1977). Blood glucose levels in portal and peripheral circulation and their relation to food intake in the rat. Physiol. Behav. *19*, 303–307.
71. Langhans, W., Grossmann, F., and Geary, N. (2001). Intrameal hepatic-portal infusion of glucose reduces spontaneous meal size in rats. Physiol. Behav. *73*, 499–507.
72. Niijima, A. (1983). Glucose-sensitive afferent nerve fibers in the liver and their role in food intake and blood glucose regulation. J. Auton. Nerv. Syst. *9*, 207–220.
73. Tordoff, M.G., and Friedman, M.I. (1986). Hepatic portal glucose infusions decrease food intake and increase food preference. Am. J. Physiol. *251*, R192–R196.
74. Tordoff, M.G., Tluczek, J.P., and Friedman, M.I. (1989). Effect of hepatic portal glucose concentration on food intake and metabolism. Am. J. Physiol. *257*, R1474–R1480.
75. Donovan, C.M., Cane, P., and Bergman, R.N. (1991). Search for the hypoglycemia receptor using the local irrigation approach. Adv. Exp. Med. Biol. *291*, 185–196.
76. Donovan, C.M., Halter, J.B., and Bergman, R.N. (1991). Importance of hepatic glucoreceptors in sympathoadrenal response to hypoglycemia. Diabetes *40*, 155–158.
77. Lamarche, L., Yamaguchi, N., and Péronnet, F. (1996). Selective hypoglycemia in the liver induces adrenomedullary counterregulatory response. Am. J. Physiol. *270*, R1307–R1316.

Please cite this article in press as: McDougle et al., Separate gut-brain circuits for fat and sugar reinforcement combine to promote overeating, Cell Metabolism (2023), https://doi.org/10.1016/j.cmet.2023.12.014

78. Delaere, F., Duchampt, A., Mounien, L., Seyer, P., Duraffourd, C., Zitoun, C., Thorens, B., and Mithieux, G. (2012). The role of sodium-coupled glucose co-transporter 3 in the satiety effect of portal glucose sensing. Mol. Metab. *2*, 47–53.

79. Fujita, S., and Donovan, C.M. (2005). Celiac-superior mesenteric ganglionectomy, but not vagotomy, suppresses the sympathoadrenal response to insulin-induced hypoglycemia. Diabetes *54*, 3258–3264.

80. Niijima, A. (1982). Glucose-sensitive afferent nerve fibres in the hepatic branch of the vagus nerve in the guinea-pig. J. Physiol. *332*, 315–323.

81. Broberger, C., Holmberg, K., Kuhar, M.J., and Hökfelt, T. (1999). Cocaine- and amphetamine-regulated transcript in the rat vagus nerve: A putative mediator of cholecystokinin-induced satiety. Proc. Natl. Acad. Sci. USA *96*, 13506–13511.

82. Li, M., Tan, H.-E., Lu, Z., Tsang, K.S., Chung, A.J., and Zuker, C.S. (2022). Gut–brain circuits for fat preference. Nature *610*, 722–730.

83. Mei, N., and Garnier, L. (1986). Osmosensitive vagal receptors in the small intestine of the cat. J. Auton. Nerv. Syst. *16*, 159–170.

84. Balleine, B.W. (2019). The meaning of behavior: discriminating reflex and volition in the brain. Neuron *104*, 47–62.

85. Hart, G., Burton, T.J., and Balleine, B.W. (2022). Striatal dopamine encodes the relationship between actions and reward.

86. de Araujo, I.E., Ferreira, J.G., Tellez, L.A., Ren, X., and Yeckel, C.W. (2012). The gut-brain dopamine axis: a regulatory system for caloric intake. Physiol. Behav. *106*, 394–399.

87. de Araujo, I.E., Lin, T., Veldhuizen, M.G., and Small, D.M. (2013). Metabolic regulation of brain response to food cues. Curr. Biol. *23*, 878–883.

88. Johnson, P.M., and Kenny, P.J. (2010). Dopamine D2 receptors in addiction-like reward dysfunction and compulsive eating in obese rats. Nat. Neurosci. *13*, 635–641.

89. Salamone, J.D., Correa, M., Yang, J.-H., Rotolo, R., and Presby, R. (2018). Dopamine, effort-based choice, and behavioral economics: basic and translational research. Front. Behav. Neurosci. *12*, 52.

90. Chong, T.T.J., Bonnelle, V., Manohar, S., Veromann, K.-R., Muhammed, K., Tofaris, G.K., Hu, M., and Husain, M. (2015). Dopamine enhances willingness to exert effort for reward in Parkinson's disease. Cortex *69*, 40–46.

91. Yu, B.M., Cunningham, J.P., Santhanam, G., Ryu, S.I., Shenoy, K.V., and Sahani, M. (2009). Gaussian-process factor analysis for low-dimensional single-trial analysis of neural population activity. J. Neurophysiol. *102*, 614–635.

92. Liu, C., Kershberg, L., Wang, J., Schneeberger, S., and Kaeser, P.S. (2018). Dopamine secretion is mediated by sparse active zone-like release sites. Cell *172*, 706–718.e15.

93. Tritsch, N.X., and Sabatini, B.L. (2012). Dopaminergic modulation of synaptic transmission in cortex and striatum. Neuron *76*, 33–50.

94. Barbera, G., Liang, B., Zhang, L., Gerfen, C.R., Culurciello, E., Chen, R., Li, Y., and Lin, D.T. (2016). Spatially compact neural clusters in the dorsal striatum encode locomotion relevant information. Neuron *92*, 202–213.

95. Markowitz, J.E., Gillis, W.F., Beron, C.C., Neufeld, S.Q., Robertson, K., Bhagat, N.D., Peterson, R.E., Peterson, E., Hyun, M., Linderman, S.W., et al. (2018). The striatum organizes 3D behavior via moment-to-moment action selection. Cell *174*, 44–58.e17.

96. Maltese, M., March, J.R., Bashaw, A.G., and Tritsch, N.X. (2021). Dopamine differentially modulates the size of projection neuron ensembles in the intact and dopamine-depleted striatum. eLife *10*, e68041.

97. Small, D.M., and DiFeliceantonio, A.G. (2019). Processed foods and food reward. Science *363*, 346–347.

98. DiFeliceantonio, A.G., Coppin, G., Rigoux, L., Edwin Thanarajah, S., Dagher, A., Tittgemeyer, M., and Small, D.M. (2018). Supra-additive effects of combining fat and carbohydrate on food reward. Cell Metab. *28*, 33–44.e3.

99. Kopp, W. (2019). How western diet and lifestyle drive the pandemic of obesity and civilization diseases. Diabetes Metab. Syndr. Obes. *12*, 2221–2236.

100. de Araujo, I.E., Schatzker, M., and Small, D.M. (2020). Rethinking food reward. Annu. Rev. Psychol. *71*, 139–164.

101. El-Sherbeni, A.A., Stocco, M.R., Wadji, F.B., and Tyndale, R.F. (2020). Addressing the instability issue of dopamine during microdialysis: the determination of dopamine, serotonin, methamphetamine and its metabolites in rat brain. J. Chromatogr. A *1627*, 461403.

Please cite this article in press as: McDougle et al., Separate gut-brain circuits for fat and sugar reinforcement combine to promote overeating, Cell Metabolism (2023), https://doi.org/10.1016/j.cmet.2023.12.014

STAR★METHODS

KEY RESOURCES TABLE

REAGENT or RESOURCE	SOURCE	IDENTIFIER
Antibodies		
Rabbit anti-c-Fos	Cell Signalling Technologies	Cat #2250; RRID: AB_2247211
Donkey anti-rabbit AlexaFluor647	ThermoFisher	Cat #A32795, RRID: AB_2762835
Bacterial and virus strains		
AAVPHP.S-FLEX-tdTomato	Addgene	Addgene viral prep #28306-PHP.S; http://n2t.net/addgene:28306; RRID:Addgene_28306
AAV5-FLEX-taCasp3-TEVp	Addgene	Addgene viral prep # 45580-AAV5; http://n2t.net/addgene:45580; RRID:Addgene_45580
AAV9-EF1a-DIO-hCHR2(H134R)-EYFP-WPRE-HGHpA[51]	Addgene	Addgene viral prep #20298-AAV9; http://n2t.net/addgene:20298; RRID:Addgene_20298
AAVrg-EF1a-mCherry-IRES-Cre	Addgene	Addgene viral prep #55632; http://n2t.net/addgene:55632; RRID:Addgene_55632
Chemicals, peptides, and recombinant proteins		
4-hydroxytamoxifen	Sigma Aldrich	Cat #H6278-50MG
CCK-saporin and saporin	Advanced Targeting Systems	Cat #IT-31 (CCK-SAP) Cat #IT-21 (SAP)
CCK Octapeptide, sulfated	Tocris	Cat #1166
Clozapin N-oxide (CNO)	Enzo Life Sciences	Cat #BML-NS105-0025
Microlipid	Nestle Health Science	Cat #9519922
Sucrose	Sigma Aldrich	Cat #S7903)
0.9% sodium chloride	Baxter Healthcare Corporation	Cat #2B1322
Critical commercial assays		
RNAscope® Multiplex Fluorescent Detection Kit v2	Advanced Cell Diagnostics	Cat #323110
Experimental models: Organisms/strains		
Mouse: C57BL/6J	The Jackson Laboratory	JAX: 000664
Mouse: B6.129(Cg)-Fos$^{tm1.1(cre/ERT2)Luo}$/J	The Jackson Laboratory	JAX: 021882
Mouse: B6.Cg-Gt(ROSA)26Sor$^{tm14(CAG-tdTomato)Hze}$/J	The Jackson Laboratory	JAX: 007914
Mouse: B6.Cg-Snap25$^{tm3.1Hze}$/J	The Jackson Laboratory	JAX: 025111
Oligonucleotides		
Cckar-c3 RNAscope probe	Advanced Cell Diagnostics	Cat #313751-C3
Penk-C2 RNAscope probe	Advanced Cell Diagnostics	Cat #318768-C2
Software and algorithms		
PRISM 10	GraphPad	https://www.graphpad.com/features
Clarity Chromatography Software	DataApex	https://www.dataapex.com/product/clarity-std
Prairie View Imaging	Bruker	https://www.bruker.com/en/products-and-solutions/fluorescence-microscopy/multiphoton-microscopes/ultima-in-vitro.html
MassLynx	Waters	https://www.waters.com/nextgen/us/en/products/informatics-and-software/mass-spectrometry-software/masslynx-mass-spectrometry-software/masslynx-quantitation-applications.html

(*Continued on next page*)

Please cite this article in press as: McDougle et al., Separate gut-brain circuits for fat and sugar reinforcement combine to promote overeating, Cell Metabolism (2023), https://doi.org/10.1016/j.cmet.2023.12.014

Continued

REAGENT or RESOURCE	SOURCE	IDENTIFIER
Other		
2018 Teklad Global 18% Rodent Diet	Inotiv	Cat #2018
Pinports, 22Ga	Instech Labs	Cat #PNP3F22
2mm CMA-7 microdialysis probes	CMA Microdialysis	Cat #P000083
Lickometer boxes and sound attenuating cubicle	MedAssociates	N/A
HTEC-510 HPLC unit	Eicom	https://www.eicom.co.jp/en/htec-510
ACQUITY UPLC HSS T3 VanGuard Pre-column	Waters	Cat #186003539

RESOURCE AVAILABILITY

Lead contact

Further information and requests for resources and reagents should be directed to and will be fulfilled by the lead contact, Guillaume de Lartigue (gdelartigue@monell.org).

Materials availability

This study did not generate new unique reagents.

Data and code availability

This paper does not report original code. Any additional information required to reanalyze the data reported in this paper is available from the lead contact upon request.

EXPERIMENTAL MODEL DETAILS

Animals

All animal procedures followed the ethical guidelines and all protocols were approved by the Institutional Animal Care and Use Committee (IACUC) at the University of Florida (Protocol # 201810305) and Monell Chemical Senses Center (Protocol # 1190). Adult mice (6-20 weeks of age, both males and females) were used and maintained on a reverse 12-h light/dark cycle while housed at 22°C with *ad libitum* access to standard rodent chow (3.1 kcal/g, Teklad 2018, Envigo, Sommerset, NJ) unless otherwise stated. We did not observe significant sex differences between male and female mice in our experiments. All mice were on a C57BL/6J background, and transgenic genotypes validated by PCR. Strain details and number of animals in each group are as follows: C57BL/6J wild type: n=62: 31 male, 31 female; bred in house, Fos^{TRAP} n=70: 35 male, 35 female; Jax B6.129(Cg)-$Fos^{tm1.1(cre/ERT2)Luo}$/J (JAX stock no.021882), Fos Cre x tdTomato: n=116: 58 male, 58 female; bred in-house from Jackson Laboratory B6.129(Cg)- $Fos^{tm1.1(cre/ERT2)Luo}$/J (JAX stock no.021882) and Ai14 (B6.Cg-Gt(ROSA)26$Sor^{tm14(CAG-tdTomato)Hze}$/J, JAX stock no.007914), and Fos Cre x tdTomato x $Snap25^{GCAMP6s}$: n=20, 10 male, 10 female; bred in-house from Jackson Laboratory B6.129(Cg)- $Fos^{tm1.1(cre/ERT2)Luo}$/J (JAX stock no.021882), B6.Cg-Gt(ROSA)26$Sor^{tm14(CAG-tdTomato)Hze}$/J (JAX stock no.007914), and Snap25-2A-GCaMP6s-D (B6.Cg-$Snap25^{tm3.1Hze}$/J, JAX stock no.025111). Prior to experiments, mice were habituated for 2–3 days to experimental conditions such as handling, injections, attachment of gastric catheter infusion pumps, behavior chambers, attachment to patch cords for optogenetics.

METHOD DETAILS

TRAP protocol

In the TRAP protocol, mice were fasted 6 hours prior to intragastric infusion. 30 min before dark onset, mice received 500 μL intragastric infusate at 100 μL/minute in the home cage. 3 h after the stimulus, mice were injected with 4-hydroxytamoxifen (4-OHT; 30 mg/kg, i.p.; MilliporeSigma, Burlington, MA), and normal chow returned to them 3 h after injection of 4-OHT. Intragastric infusates were saline, sucrose solution (75%, 30%, or 15% w/v), an equicaloric fat solution (33.3%, 13.4%, 6.8% v/v; Microlipid, Nestle, Vevey, Switzerland), or an equicaloric combined solution of 50% fat and 50% sugar by caloric content. The osmolarity of saline was matched to the different concentrations of sucrose. There was negligible difference in the viscosity of microlipid and sucrose. Prior work from our lab demonstrates that the palatability of fat and sucrose are not a driving factor in the consumption of vagal mediated fat and sugar intake.[56]

Surgeries

Nodose ganglia (NG) injection

Ten minutes before surgery, mice received a subcutaneous injection of carprofen (5 mg/kg; Henry Schein). Mice were anesthetized with 1.5-2.5% isoflurane, a 2 cm midline incision was made in the skin on the ventral aspect of the neck, underlying muscles, salivary

Please cite this article in press as: McDougle et al., Separate gut-brain circuits for fat and sugar reinforcement combine to promote overeating, Cell Metabolism (2023), https://doi.org/10.1016/j.cmet.2023.12.014

glands and lymph nodes were retracted, and the vagus nerve was separated from the carotid artery by blunt dissection using fine-tip forceps. The NG was located by tracing the vagus nerve toward the head, and then exposed by retracting surrounding muscles and blunt dissection of connective tissues. A glass micropipette (30 μm tip diameter, beveled 45 degree angle) filled with either of the viral constructs (pAAV9-Ef1a-double floxed-hChR2(H134R)-EYFP-WPRE-HGHpA (Addgene 20298), pAAV5-flex-taCasp3-TEVp (Addgene 45580), pAAV.Php.S-FLEX-tdTomato (Addgene 28306), Addgene, Watertown, MA), CCK-saporin (ATS Bio, Carlsbad, CA), or saporin (ATS Bio, Carlsbad, CA) attached to a micromanipulator was used to position and puncture the NG. A Picospritzer III injector (Parker Hannifin, Pine Brook, NJ) was used to control injection speed and volume directly into the NG (total volume 0.5 μl). Incision was closed using 5-0 absorbable sutures in a running stitch and at 24 hours post-op analgesic was administered. Mice were fed with moistened chow and given at least 2 weeks for recovery and viral expression prior to experimentation. pAAV5-flex-taCasp3-TEVp was a gift from Nirao Shah and Jim Wells (Addgene viral prep # 45580-AAV5; http://n2t.net/addgene:45580; RRID:Addgene_45580), pAAV-FLEX-tdTomato was a gift from Edward Boyden (Addgene viral prep # 28306-PHP.S; http://n2t.net/addgene:28306; RRID:Addgene_28306) pAAV-EF1a-double floxed-hChR2(H134R)-EYFP-WPRE-HGHpA was a gift from Karl Deisseroth (Addgene viral prep # 20298-AAV9; http://n2t.net/addgene:20298; RRID:Addgene_20298), and AAV-Ef1a-mCherry-IRES-Cre was a gift from Karl Deisseroth (Addgene plasmid # 55632-AAVrg; http://n2t.net/addgene:55632; RRID:Addgene_55632).

Retro Cre HPV application

In mice anesthetized with 1.5 - 2% isoflurane, analgesics buprenorphine XR 1 mg/kg and carprofen 5 mg/kg were administered subcutaneously 20 min prior to the surgery. An abdominal laparotomy, typically 1.5 cm, was performed. The liver was retracted to expose the HPV, and sterile parafilm was placed over the region with a fenestration over the HPV, to prevent spread of the viral vector. The viral retrograde vector (pAAVrg-Ef1a-mCherry-IRES-Cre, Addgene 55632; 1 μL per mouse) was applied with a small, sterile paintbrush to the HPV, brushing vigorously to ensure viral penetration. Incision site was closed with 5-0 suture for the peritoneum, and wound clips for the skin and at 24 h post-op analgesic (carprofen) was administered. Mice were fed with moistened chow and given at least 2 weeks for recovery and viral expression prior to experimentation.

Intragastric (IG) catheter implantation

IG catheters consisted of 6 cm silicon tubing (.047" OD x.025" ID, SIL047, Braintree Scientific, Braintree, MA) with 6 beads of silicon glue (#31003, Marineland, Blacksburg, VA) applied at 1 mm, 3 mm, 13 mm, and 15 mm from the distal end, and at 10 mm and 12mm from the proximal end, and a Pinport (Instech Labs, Plymouth Meeting, PA) for chronic intermittent access. In anesthetized mice, a 1.5 cm laparotomy was made, and the stomach externalized using blunt forceps and sterile cotton swabs. A 4 mm purse-string suture was made with 5-0 absorbable suture at the junction of the greater curvature and fundus, avoiding major blood vessels. The center of the purse-string was punctured with an 18-gauge needle, and the catheter is pushed in until the first bead of silicone glue is inside the stomach, the second bead exterior. The purse-string suture was then tightened and tied, anchoring stomach wall between the two beads of silicon glue. Next, a hole was punctured in the left lateral abdominal wall and fine-tip forceps used to pull the catheter through until the peritoneal wall was between the third and fourth beads of silicone glue. A purse-string suture was made in the peritoneum around the catheter, tightened and tied to anchor the catheter to the peritoneum between the two beads of glue. The peritoneum laparotomy was closed with 5-0 absorbable suture. A 2 mm midline dorsal cutaneous incision was made caudal to the interscapular area, and a sterile blunt probe, 1 mm by 14 cm inserted and tunneled under the skin caudal to the left foreleg, to the abdominal incision. The catheter was threaded onto the end of the blunt probe and pulled through until the first bead on the proximal end is externalized, with the second proximal bead under the skin. The end of the tubing was cut off just above the external bead and a 22-gauge Pinport secured in the tube with superglue. A purse-string suture was made around the catheter, anchoring it to the skin between the two silicone beads. The abdominal incision was closed with suture clips. Analgesics buprenorphine XR (1 mg/kg) and carprofen (5 mg/kg) were administered subcutaneously 20 min prior to surgery and carprofen again at 24 h post-op. Mice were fed with moistened chow and given at least 1 week for recovery prior to experimentation. Daily body weight was monitored until pre-surgical weight was regained.

Vagotomy

Surgeries were performed aseptically following the IACUC Guidelines for Rodent survival surgery. Mice were anesthetized by inhalation of a continuous flow of 1.5-2.5% isoflurane. The pedal reflex test was performed prior to surgery to ensure that each mouse had reached an appropriate level of anesthesia. Mice were placed on a sterile drape warmed by a heating pad. Fur was shaved from the abdomen before cleansing with three exchanges of EtOH and Betadine. Sterile surgical equipment was used to create a 2-4cm midline laparotomy. The small intestine and colon were externalized and placed on sterile gauze moistened with sterile 0.9% NaCl saline. The subdiaphramatic vagus nerve was visualized by gentle retraction of the liver and stomach. Complete vagotomy was performed by cutting the left and right cervical branches of the vagus directly caudal of the diaphragm using spring scissors. Hepatic sparing vagotomy was performed by cutting the subdiaphragmatic right cervical vagus nerve directly caudal of the diaphragm and the subdiaphragmatic left cervical vagus nerve caudal of the common hepatic branch and rostral to the lower esophageal sphincter. Sham animals had their subdiaphragmatic vagus nerve visualized, isolated, but not cut. The internal organs were repositioned and the incision site was covered with sterile gauze moistened with 0.9% saline.

Following the vagotomy, a silicone tubing was inserted via a small opening in the stomach wall, into the proximal section of the duodenal lumen. The duodenum received a 2-minute infusion of 200 μL sucrose (15% v/w). Post-stimulation, incisions were sutured, and the mice were allowed to recover on a heating pad until they voluntarily moved to the unheated section of the cage. After 90 minutes, the mice were perfused and brains harvested, post-fixed in 4% PFA for 24 hours, and kept at 4 °C in a 30% sucrose in PBS solution until processing.

Please cite this article in press as: McDougle et al., Separate gut-brain circuits for fat and sugar reinforcement combine to promote overeating, Cell Metabolism (2023), https://doi.org/10.1016/j.cmet.2023.12.014

In vivo 2-photon imaging

We used a 2-Photon microscope (Bruker) fitted with a Galvanometer for acquisition, and a piezo objective combined with a galvo/resonant scanner that allowed images to be obtained at a frame rate of 29 frames/second. The microscope was set up for *in vivo* imaging with a Somnosuite (isoflurane) anesthesia machine coupled to a homeothermic control warm pad (Kent Scientific) and a Programmable Syringe pump (Harvard apparatus PHD 2000, Cat no. 70-2002) for infusing nutrients in the gut.

Mice fasted for at least 2 h after the onset of dark were placed under continuous anesthesia (1.5% isofluorane) and kept on a heating pad to maintain body temperature throughout the whole procedure. An incision (~2 cm) was made above the sternum and below the jaw, the carotid and vagus nerve were exposed after separation of the salivary glands. Retractors were used to pull the sternomastoid, omohyoid and posterior belly of digastric muscle sideways and make the NG visible. The vagus nerve was cut immediately above the NG, which was carefully separated from the hypoglossal nerve and small adjacent branches. The vagus nerve was then dissected from the carotid and surrounding soft tissues, and the right NG was gently placed on a stable imaging platform consisted of an 8 mm diameter coverslip attached to a metal arm affixed to a magnetic base. Surgical silicone adhesive (Kwik-Sil, WPI) was applied onto the vagus nerve to keep it immobilized on the coverslip and the NG immersed in a drop of DMEM (Corning) media was covered with a second coverslip. Imaging was performed) using a 20x, water immersion, upright objective.

Infusions were performed with a precision pump that held syringes attached to a silicone tubing and filled with either sucrose, corn oil (Mazola) or saline. Prior to surgery to expose the NG, a small abdominal incision was made of the anesthetized mouse to expose the stomach. Next, the silicone tubing was inserted through a small incision in the stomach wall, into the proximal portion of the duodenal lumen. In some animals an exit port was created ~2 cm distally to pylorus by transecting the duodenum. Super glue was applied onto the wall of the stomach to prevent the tubbing from sliding out of the intestine. To determine that there are distinct nutrient responsive subpopulations in the NG, neuronal activity of in response to different stimulus was monitored within the same mouse. Recordings of baseline neuronal activity signals started with continuous infusion of saline for 1 min (100 μl/min) followed by 5 minutes of 75% w/v sucrose infusion (100 μl/min), and then additional 10 min of saline flush (100 μl/min) to clear out the sucrose residues from the exit port. This was followed by the recording of a second baseline within the same animal after infusion of saline for 1 min (100 μl/min) followed by 5 min of corn oil (100%) infusion (100 μl/min). In a separate cohort of Fos^{TRAP}:Ai14 x $SNAP25^{GCaMP6s}$ mice, trapped in response to intragastric infusion of sucrose (15% w/v). The right NG of mice was exposed as described above and recorded during intragastric saline infusion as baseline and for 15 minutes in response to 5 minute intragastric infusion of sucrose (15%) or equicaloric microlipid (6.8%) without an exit port. The latter experimental design matches that used during the TRAP procedure, and mimics more naturalistic feeding conditions overcoming potential issues associated with presentation order resulting in altered circulating glucose levels.

GCaMP6s fluorescent changes were outlined in regions of interests (ROIs) with each ROI defining a single cell throughout the imaging session. The pixel intensity in ROIs (average across pixels) were calculated frame by frame (ImageJ) and exported to excel for manual analysis. The baseline signal was defined as the average GCaMP6s fluorescence over 5 min (fat or sucrose or saline) period prior to the stimulus introduction. Cells were considered responsive to nutrients if the following criteria were met: 1) the peak GCaMP6s fluorescence was two standard deviations above the baseline mean and 2) the mean GCaMP6s fluorescence was $\geq$ 70% above the baseline mean for a 20 second window around the peak. NG in which neurons did not present baseline activity were excluded from the study.

Stereotaxic implants and viral injections

Mice were anesthetized mice with 1.5-2.5% isoflurane and placed in a stereotaxic apparatus (World Precision Instruments, Sarasota, FL) while resting on a heating pad. After skin incision (1-1.5 cm) and removal of all soft tissue from the surface of the skull, the periosteum was removed by blunt dissection. A dental drill was used to penetrate the skull above the target area. The skin was closed with 5-0 absorbable suture.

For optogenetic post implants, the holes were drilled (0.6-1 mm) nearby and stainless-steel screws secured allowing better fixation of the probe. Optogenetic posts were composed of fiber optic (FT200UMT, Thorlabs, Newton, NJ) secured in a ceramic ferrule (LC Zirconia Ferrule FZI-LC-230, Kientec, Stuart, FL) with UV-cured adhesive (RapidFix, St. Louis, MO). Posts were implanted over vagal terminals in the NTS (AP: -7.5mm, ML: ± 0.3mm, DV -5.0mm) and secured with dental cement (GC Fujicem 2, GC America, Tokyo, Japan). Dental cement was used to cover the exposed skull, including screws, and allowed to set completely before mice were moved to the recovery area.

For microdialysis implants, the same protocol above was performed, except microdialysis guide cannulas (Amuza, San Diego, CA) were implanted in the DS as validated previously[22] (AP:+1.5, ML: ±1.5, DV:-3.0). An obturator or dummy cannula was used to keep the guide cannula patent, protruding at least 1 mm on the ventral side and the dorsal side screwed to the guide cannula thread.

Behavioral Tests

Food restriction

During all behavioral experiments, mice were maintained at 85-90% of body weight by restricting access to food. Briefly, for weight maintenance, approx. 2-3 g of food (10% of body weight) were given to mice 2 h after completion of the behavioral task. This paradigm ensured that mice learn to distinguish nutrients paired with the test solution without being confounding the association by any undigested chow in the gastrointestinal tract. In all cases, body weight was assessed every 24 h, just prior to refeeding. If any mouse weighed less than 85% of their starting body weight, they were fed 2.5 g plus the excess weight loss in g until they reached 85% of starting body weight again. *Ad libitum* water access was provided in home cage.

Please cite this article in press as: McDougle et al., Separate gut-brain circuits for fat and sugar reinforcement combine to promote overeating, Cell Metabolism (2023), https://doi.org/10.1016/j.cmet.2023.12.014

Behavioral apparatus

All behavioral experiments - in conjunction with optogenetic stimulation and/or CNO infusions - were conducted in mouse behavioral chambers enclosed in a ventilated and sound attenuating cubicle (Med Associates Inc., St. Albans, VT). Each chamber was equipped with slots for sipper tubing equipped with contact lickometers with 10 ms resolution (Med Associates Inc.) used for licking detection. Separate chambers with a 5-hole nose poke wall with infrared beam detectors were used for nose-poke operant tasks (Med Associates Inc). These chambers were used in conjunction with optogenetic stimulation and/or pump-controlled infusion through a gastric catheter.

Flavor-nutrient conditioning task

Food restricted mice were placed in soundproof operant lickometer boxes (Med Associates) for training and habituation with one bottle of 0.2% w/v saccharin for 1 h per day for at least 3 consecutive days or until mice licked at least 1,000 times per h. Each day the bottle was placed in the right or left-hand sipper slot to avoid formation of a side preference. Once mice were trained to lick from the sippers, they underwent a pre-test, in which they were given 10-min access to two artificially sweetened (0.025% w/v saccharin) Kool-Aid (0.05% w/v) flavors in Med Associates lickometer boxes, one on the right and one on the left. At the 5-min point, the flavor positions were swapped to minimize the effects of individual side preference. The total number of licks for each flavor was tallied across the session and the nutrient (positive conditioned stimulus) was paired to the less preferred flavor and saline to the more preferred flavor to avoid a ceiling effect on preference for the nutrient-paired flavor. Flavor-nutrient pairings were counterbalanced within groups. After the pre-test, mice underwent 1-h conditioning sessions on 6 consecutive days, receiving access to a flavor with intragastric solution of either saline or nutrient on alternating days. To avoid the formation of a side preference during conditioning, mice received each flavor for an equal amount of time on each side of the box, alternating every 2 days. After 6 days of conditioning, on post-test day, a 10-min 2-bottle preference test was repeated in the absence of intragastric infusions, exactly as during the pre-test. Outcomes were measured by the percent preference each subject had for the nutrient-paired flavor during post-test.

Nose-poke self-stimulation

Mice were trained to nose-poke for optogenetic stimulation in a Med Associates nose poke chamber with 2 nose-pokes, one active and one active following our previously published protocol.[22] Mice were randomly assigned right or left active nose-pokes in a counterbalanced manner and underwent 3 days of 30-min nose-poke training during which a small amount of powdered rodent chow was placed in both nose pokes to motivate mice to explore the nose pokes. During all sessions, mice were tethered to a fiber-optic cable with swivel attached to laser and active nose-pokes resulted in optogenetic stimulation at 1 Hz frequency for 1 s duration at 5 mW intensity (measured at the fiber tip), as previously validated.[22] Following 3 days of training, mice underwent 3 days of testing without food in the nose-pokes, during which the number of active and inactive nose pokes was measured over a 30-min test period each day.

Microdialysis experiments

All mice were acclimated to microdialysis chambers for 4 h for 3- 4 days before the experiment day to reduce handling stress and neophobia. On the first day of microdialysis experiment, the cap of the guide cannula was removed, and a dialysis probe inserted into the guide cannula. After probe insertion, each mouse was placed in a microdialysis chamber and allowed to acclimate for 2 h with water available *ad lib*. Microdialysate samples were then collected for 4 h while the animal was allowed to freely move around the cage. The dialysis probe was connected to an infusion pump by flexible Tygon tubing surrounded by a flexible spring tether attached to a liquid swivel and was perfused with artificial cerebrospinal fluid (aCSF) at a flow rate of 1 μl/min throughout the experiment. The tether was long enough for the animal to reach all parts of the test box unencumbered so that mice could comfortably sleep or drink while attached to the tether. Sample collection continued during intragastric infusion of nutrients and for 1-2 h afterwards. Each animal received a maximum of 3 different stimuli (saline, fat, and either sugar or combo) this allowed within animal comparisons. We infused 2-3 different stimuli per day with a 1-h interval between saline and stimuli over a 3-day period, with 3 days of recovery between tests.

During experimental sessions, microdialysate samples from freely moving mice were collected, separated, and quantified by HPLC coupled to electrochemical detection methods ("HPLC-ECD"). Briefly, a microdialysis probe (2 mm CMA-7, cut off 6kDa, CMA Microdialysis, Stockholm, Sweden) was inserted into the striatum through the guide cannula (the corresponding CMA-7 model). After insertion, probes were connected to a syringe pump and dialysates collected. Dopamine was detected using an HTEC-510 HPLC unit (Eicom, San Diego, CA) presented in Figure 4 or UPLC-coupled spectrometry presented in Figure 5.

For data in Figure 4, DS was perfused at 1.2 μl/min with artificial CSF (Harvard Apparatus). After a 2 h washout period, dialysate samples were collected every 7 min and frozen. Analytes were separated by injecting samples using an autosampler into a cation exchange column (CAX, Eicom), and detected with an electro-chemical detector (+450mV, 250ul/min) resulting chromatograms were analyzed using the software Clarity (DataApex). Actual sample concentrations were computed based on peak areas obtained from 0.5 pg/μl DA standards (Sigma) and expressed as % changes with respect to the mean DA concentration associated with baseline samples.

For data in Figure 5, microdialysates were collected in 15 min bins (aCSF at 1 μl/min rate) for 1-h after saline infusion (500 μl at 100 μl/min rate) and then for 1-h after nutrient first stimuli infusion (either combo of 3.4% fat and 7.5% sugar or isocaloric 6.8% fat; 500 μl at 100 μl/min rate) and followed by another saline infusion and the second stimuli for the subsequent 2-h. Microdialysate was collected in a 15 μL cocktail of EDTA (50 μg/mL), L-ascorbic acid (45 μg/mL), and acetic acid (0.05% v/v) in aCSF and frozen on dry ice.[101] For sample processing, microdialysate (20 μL) samples were diluted with methanol (0.05% acetic acid; 20 μL) containing

Please cite this article in press as: McDougle et al., Separate gut-brain circuits for fat and sugar reinforcement combine to promote overeating, Cell Metabolism (2023), https://doi.org/10.1016/j.cmet.2023.12.014

internal standard (Dopamine-d4; 25 ng/mL), vortex mixed, filtered through a multiscreen Solvinert (Millipore, St. Louis, MO) 96-well filter plate (0.45 μm), centrifuged (2000g, 5 min, 4°C), and injected onto Waters Acquity UPLC coupled with Xevo® TQ-S micro triple quadruple mass spectrometer. Waters ACQUITY UPLC HSS T3 (100 × 2.1, 1.8 μm) with a VanGuard pre-column of a comparable chemistry (Waters Co, Milford, MA) was used to achieve chromatographic separation in gradient mode. The optimized linear gradient program includes 0.1% formic acid in water (mobile phase A) and methanol (mobile phase B) and was as follows: 0–0.8 min, 5% B; 0.8–1.5 min, 5-25% B; 1.5–2.5 min, 25% B; 2.5–2.6 min, 25–5% B; 2.6–3.0 min, 5% B. A blank aCSF containing EDTA (50 μg/mL), L-ascorbic acid (45 μg/mL), and acetic acid (0.05%, v/v) was spiked with known amounts of dopamine to prepare calibration and quality control standards. Actual sample concentrations were computed based on peak areas obtained from 0.1 pg/μl DA standards (Sigma) and expressed as % changes with respect to the mean DA concentration associated with baseline samples.

Perfusions

Anesthetized animals were transcardially perfused with phosphate buffer saline (PBS) until all blood was cleared, followed by cold 4% paraformaldehyde (PFA) in PBS for 2 minutes using the Leica Perfusion One System (Leica Biosystems, Wetzlar, Germany). Tissues including brain, NG, stomach, intestine, and HPV, were then harvested, post-fixed for 24 h in 4% PFA in PBS, before being transferred to 30% sucrose with 0.1% sodium azide for a minimum of 72 h before processing.

Tissue processing & storage

Slicing

Whole brains were embedded in OCT and sliced in 1 in 3 series at 35 μm thickness on a Leica frozen microtome (CM 3050 S, Leica Biosystems) kept at -20°C. Slices were stored in cryoprotectant at -80°C until further staining or imaging. Nodose ganglia were embedded in OCT (Sakura, Torrance, CA) and sliced at 15 μM and frost mounted on Fisherbrand Superfrost Plus slides (Fisher Scientific) in 1 in 3 series and stored at -20°C until further processing.

Immunohistochemistry – Fos

Tissue was removed from cryoprotectant and rinsed 3 times for 10 min each in PBS at room temperature in 6-well plates, before being incubated for 30 minutes in blocking solution consisting of permeabilizing agent (244.5 mL PBS, 5 mL serum, 0.5 mL Triton-X100, 0.25 g Bovine Serum Albumin) and 20% normal donkey serum to prevent non-specific antibody binding. Tissue was then incubated overnight in permeabilizing agent with 1:1000 cFos antibody (Cell Signaling Technologies, rabbit-anti-cFos #2250) at room temperature. The next day, tissue was rinsed in PBS 3 times for 20 min each to remove unbound antibody, then incubated 2 h in permeabilizing agent containing 1:1000 secondary antibody (Donkey-anti-rabbit Alexafluor 647; AbCam, Cambridge, UK). Tissue was then rinsed 3 times for 2 h each in PBS, mounted onto plus slides, coverslipped with Prolong Diamond Antifade Mountant (Invitrogen, Waltham, MA), and stored at -20 °C until imaging and analysis.

Tissue clearing

To image the vagal terminals in peripheral tissue, the gut and HPV were cleared by incubating in TDE (2,2′-thiodiethanol, MilliporeSigma) for a minimum of 2 h prior to imaging.

RNAscope NTS and NG

We employed RNAscope for Single-Molecule fluorescence in-situ hybridization using a fluorescent multiplex kit (Advanced Cell Diagnostics) in NG and NTS sections (15μm and 20μm thickness respectively). Specifically, we employed C2 and C3 DNA oligonucleotide probes for the specific genes Penk-C2 and Cckar-C3. Our experimental procedure comprised the following steps: Tissue sections were post-fixed using a 4% paraformaldehyde solution for a period of 15minutes, and underwent sequential ethanol washes (5min 50%, 70%, 100% and an additional 100%). The sections were air-dried for 5 min, and washed for 10 minutes in hydrogen peroxide. For NTS sections an additional target retrieval step was performed. Protein digestion was performed (protease III for brain sections and protease IV for NG sections) at 40°C for 30 minutes and washed twice with distilled water. Subsequently, the Penk-C2 (for NTS) or Cckar-C3 (for NG) probes were applied to the slides and stored in a humidified incubator at 40°C for 2 hours. The slides were rinsed twice in an RNAscope wash buffer, and the subsequent steps involving colorimetric reactions were performed in accordance with the standardized protocol provided within the kit (OPAL- Akoya Biosciences, Marlborough, USA). After the final wash buffer step, the slides were promptly coverslipped using DAPI (4′,6-diamidino-2-phenylindole) containing Prolong Diamond Antifade mountant (Invitrogen, Waltham, MA).

Imaging

Tissue sections labelled for Fos expression or mRNA probes were imaged using a Keyence BZ-X800 in a single plane with autofocus capture at 10x, or a Leica TCS SP8 confocal microscope at 20x. Quantification of Fos expression and colocalization was conducted using merged fluorescence images from a minimum of 3 sections/region/animal. The data are expressed as the average number of positive cells per section for each group. For imaging of sections processed for in situ hybridization, positive and negative control probes were used to determine exposure time and image processing parameters for optimal visualization of mRNA signals and control for possible photobleaching. Brightness and contrast adjustment and automated quantification of Fos expression and colocalization was done with Nikon NIS Elements or Image J software.

QUANTIFICATION AND STATISTICAL ANALYSIS

Data are presented as mean ± SEM and were analyzed for statistical significance as described in figure legends using Student's t-test, Wilcoxon signed rank test, one-way within-subjects or two-way within-subjects/mixed-model analysis of variance (ANOVA)

Please cite this article in press as: McDougle et al., Separate gut-brain circuits for fat and sugar reinforcement combine to promote overeating, Cell Metabolism (2023), https://doi.org/10.1016/j.cmet.2023.12.014

(with the Greenhouse–Geisser correction applied as appropriate). Appropriate parametric or non-parametric tests were performed to evaluate statistical significance after checking the normality of the data. Significant one-way ANOVA tests were followed by pairwise comparisons with correction for multiple comparisons. For two-way ANOVA, either simple main effects were reported, or significant interactions were reported and followed by pairwise comparisons with correction for multiple comparisons. The threshold for statistical significance was $p<0.05$, and significant comparisons are reported in all figures as $^{*}p < 0.05$, $^{**}p < 0.01$, $^{***}p < 0.001$ and $^{****}p < 0.0001$. Comparisons in which $p < 0.1$ (but ≥ 0.05) are reported with exact p-values. Statistical analyses were performed in GraphPad Prism. Statistical details of experiments can be found in the figure legends and a breakdown is available in Data S1 Source data file.